Conf-9010297--2

UCRL-JC--105174

DE91 007255

NEW, HEAVY TRANSURANIUM ISOTOPES

E. K. Hulet

THIS PAPER WAS PREPARED FOR SUBMITTAL TO
PROCEEDINGS OF CONF. ON CHEMICAL RESEARCH XXXIV,
50 YEARS WITH TRANSURANIUM ELEMENTS,
Houston, TX, October 22-23, 1990

October 22, 1990

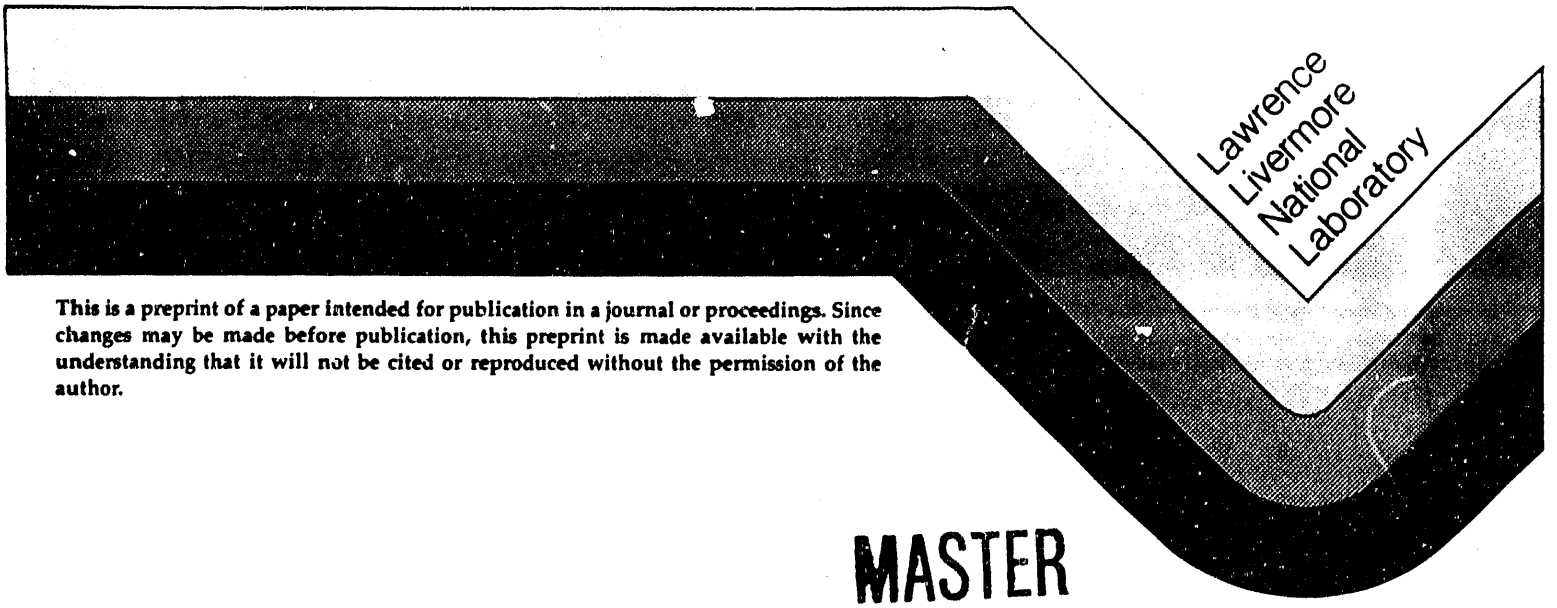

DISCLAIMER

NEW, HEAVY TRANSURANIUM ISOTOPES

E. K. Hulet

University of California, Lawrence Livermore National Laboratory
Livermore, CA 94551, USA

INTRODUCTION

Transuranium nuclei offer an extremely rich environment for the study of unusual properties and decay processes unknown in the lighter elements. Research in this region of nuclides provides fertile grounds for testing nuclear matter near its limiting conditions, where a lack of quantitative understanding of stability and of fission poses one of the outstanding remaining challenges to nuclear theory. It is for these reasons that we continue to probe in search for new, very heavy nuclides in attempts to further understand the massive rearrangements accompanying fission, the exotic decay modes, and the unusual deformations found only in this region. These searches have become increasingly arduous because of the exponential decrease in formation cross sections due to prompt fission competition and to half-lives approaching the limits of detection near a microsecond. Nevertheless, three new elements and over fourteen new isotope have been synthesized in recent years. These discoveries have caused a re-evaluation of our understanding of the fission process and provided a deeper appreciation of the role played by nuclear shells in enhancing the stability of nuclear matter near its limits.

Here, I shall discuss our group's work in the synthesis of five new, transfermium isotopes by means of transfer reactions in bombardments of ^{254}Es with heavy ions. Formation of these nuclei was virtually prohibited by any other nuclear reaction because of insufficient numbers of neutrons in available targets or projectiles. A portion of the nuclide chart, illustrated in Fig. 1, indicates the nuclear reaction paths and the products formed from bombardments of einsteinium with heavy ions.

The potential for producing new nuclides from transfer reactions of ^{18}O and ^{22}Ne with ^{254}Es were first investigated in 1981 and 1982. In these preliminary experiments, we measured the cross sections for the formation of a series of isotopes of Es, Fm, and Md by radiochemical methods. To later extend these cross section measurements to shorter-lived isotopes of Md, No

and, Lr, we employed a He-jet transfer system at the Gesellschaft für Schwerionenforschung, Darmstadt. These transfer cross sections,[1] including new ones for nuclides that were later discovered, are given in Figs. 2a and b. Considering that the isotopic yield curves for each element are Gaussian distributions, it was clear from extrapolating these curves to larger mass numbers that a number of new, neutron-rich isotopes of Md, No, and Lr could be produced with cross sections larger than 10 nb. However, transfer cross sections for producing any isotope of element 104 are expected to be below this level and none have been found so far. The extrapolations to predict the production cross sections of unknown nuclei are uncertain by less than 20 to 30%; thus, the principal restraints to identifying new isotopes in this region were largely the difficulties of the experiments. Among these is the need to devise rapid separation methods to isolate new nuclides because of the large (millibarns) cross sections for forming known nuclides near the target isotope. Otherwise, the background radiation from known nuclei would overwhelm that from the unknown. Another difficulty comes from estimating the half-lives and decay properties for undiscovered nuclides in this region. While half-lives for decay by α, β^-, and electron-capture (EC) normally can be predicted to within a factor of 2 to 3, those for spontaneous fission (SF) are too sensitive to barrier heights to be accurately estimated. Before the theoretical estimates can be improved, additional experimental SF half-lives for neutron-rich nuclei are needed

In the following, we offer our most recent results concerning the decay properties for five new isotopes of Md, No, Lr, and for ^{258m}Md. In additions to these successful experiments, we have also conducted searches for ^{263}[105], ^{264}[105], ^{272}[109], and superheavy elements from bombardments of ^{254}Es with heavy ions.[2] An exciting finding in the course of this work is a new fission phenomenon, which we have termed "bidmodal fission". This is described in a subsequent section. The final part summarizes our conclusions based on the unexpectedly long half-lives and surprising fission properties of the heaviest nuclei.

2. NEW ISOTOPES OF Md, No, AND Lr

a. ^{258m}Md

Although 51-d ^{258}Md had been found some years earlier, the first indications of a shorter lived isomer came from bombardments of 3×10^{11} atoms of ^{255}Es with 26.3-MeV α particles.[3] A spontaneous-fission (SF) activity decaying with a 43-min half-life was detected in the products of these bombardments. However, the amount produced was too low to chemically identify the source of the SF activity, but it was assumed on the basis of estimated Q values that ^{258m}Md would decay mainly by electron capture (EC) to 370-μs ^{258}Fm, which was known to decay by SF. These earlier results have been largely confirmed from our bombardments of ^{254}Es with both

^{18}O and ^{22}Ne ions in which our production rate was about 4500 times greater than with the much smaller ^{255}Es target.[4] From this new study, the half-life found for ^{258}Md from following the decay of eight mass-separated samples was 57±1 min. Because these sources were prepared by electromagnetic mass separation, the mass number of the SF activity was established. Furthermore, we have determined with certainty the element identification of 370-μs ^{258}Fm and the mother-daughter genetic relationship between ^{258m}Md and ^{258}Fm by the observation of time-correlated Fm K x-rays preceding SF by ^{258}Fm.[4] The distribution of time intervals that we obtained is shown in Fig. 3. The larger peak near 290 ms is due to random background photons that happen to fall within our photon-energy window. The peak at 520 μs corresponds to the lifetime of ^{258}Fm following its formation by EC decay of ^{258m}Md and equals a half-life of 360±20 μs. This half-life is to be compared with the value of 380±60 measured by another method in earlier discovery experiments.[5]

b. ^{260}No

A SF activity with a half-life of 106±8 ms was produced with a cross section of 1.1±0.2 μb in reactions of 99-MeV ^{18}O ions with ^{254}Es.[6] Activities with a similar half-life were made with cross sections of ≤80 and 200 nb in bombardments of ^{254}Es with 125-MeV ^{22}Ne ions and 73-MeV ^{13}C ions, respectively. Because the formation cross section from the reaction $^{18}O + ^{254}Es$ was consistent with an extrapolation of the No yield curve to mass 260, as can be seen in Fig. 2a, it was suggested this new SF activity was associated with the decay of ^{260}No. From recently compiled cross sections for 72-MeV ^{13}C transfer reactions with ^{254}Es (Fig. 4),[7] we conclude the 200-nb cross section reported by Somerville *et al.* for possibly making ^{260}No from ^{13}C appears an order of magnitude to large. Similarly, their cross section for producing this activity from ^{22}Ne transfer reactions is inconsistent, as their upper limit for the cross section seems three to four less time than expected from an extrapolation of the No yield-curve in Fig 2b. Therefore, we feel the assignment of this 100-ms activity is on shaky grounds, but it is still difficult to imagine any other alternative, especially since we have identified most of the surrounding nuclides. The large 1.1 μb cross section from ^{18}O reactions with ^{254}Es precludes isomers or nuclei more distant than ^{260}No. Everything considered, we would judge the assignment to be probable but, at the first opportunity, new experiments to prove the isotopic source of this 100-ms activity should be made.

c. ^{260}Md

From bombardments of ^{254}Es with both ^{18}O and ^{22}Ne ions, we discovered ^{260}Md in isotopically separated samples of the reaction products.[8] After collecting products recoiling from the target on Ta foils, we transported the foils from the 88-in cyclotron at the Lawrence Berkeley Laboratory to the Lawrence Livermore National Laboratory for off-line electromagnetic separation. The elapsed time from the end of bombardment until counting started after isotope separation was close to an hour. The mass-260 fraction decayed by spontaneous fission with a 27.8±0.8 day half-life (Fig.5). This same SF activity has been chemically identified many times over as belonging to the element Md. In view of the Q values for β^- decay of up to 1 MeV and, for EC, in the range of 0.5 to 1.4 MeV, we initially believed the SF activity probably originated from the possible daughters, ^{260}No or ^{260}Fm, in equilibrium with the 29-d parent. To check these possibilities, we constructed two specialized counting systems to measure the time intervals between β^- particles, K x-rays or L x-rays and a subsequent fission event. Because both daughter nuclides were predicted to have SF lifetimes of well under 1 s, these counting systems were designed to cover time intervals from about 10 ns up to 1 s. Maintaining the maximum geometrical efficiency for each type of radiation was necessary because only about 1500 atoms of ^{260}Md could be prepared per bombardment. Total efficiencies, including geometry and detector efficiencies, were 60% for β^- particles up to 0.7 MeV, 34% for K and L x rays and, for fission fragments, 61% in the β^- system and ~90% in the x-ray system. In the β^- system, surface-barrier (Au) detectors depleted to a depth of 1 mm were used to detect and measure the energies of both β^- particles and fission fragments. In a separate counting system, K- and L-x-ray energies were measured with intrinsic-Ge detectors with a resolution averaging 1.1 keV between 100 and 150 keV. We made two to three bombardment to produce ^{260}Md for each of the three counting experiments.

Analysis of our time-correlated data was complex because of background radiation whose random time distribution before fission partially overlapped the 100-ms lifetime region of potential daughters. Only in the case of β^- decay was the background rate sufficiently low to not interfere with detecting a SF daughter having a half-life of 106 ms, the period expected for ^{260}No (see above). From these experiments, our 2σ upper limit for a possible β^--decay branch by ^{260}Md, assuming a daughter lifetime of 100 ms, is 7.2%. The statistical analysis of the time intervals and photon energy data for possible K- or L-electron capture is incomplete, but the probabilities for a decay branch by either of these modes appears to be less than 15%. There was no obvious excess of photons above background with Fm $K_{\alpha 1}$ or $K_{\alpha 2}$ energies occurring 100 ms before fission and the same was also true for Fm L x-rays. Thus, we are assured that most if not all of the SF activity we observed in the mass-260 fractions arises directly from the SF decay of ^{260}Md.

During the search for possible daughters, we also measured correlated fission-fragment energies and have derived the mass and kinetic-energy distributions for SF by ^{260}Md. Because of the uncommon total-kinetic-energy distribution (TKE) and long half-life, we also determined the neutron multiplicity as a function of fragment energies. These results are described collectively in Section 3 under bimodal fission.

d. ^{261}Lr and ^{262}Lr

Experiments conducted in 1984 gave us the first indication of the existence of ^{261}Lr and ^{262}Lr from the presence of excess SF activity in the mass-261 and -262 fractions, following electromagnetic separation of the recoil products from ^{22}Ne bombardments of ^{254}Es. These fission activities decayed with roughly a 1-h half-life and disappeared entirely after about 4 hours. The cross sections and decay periods were consistent with those expected for new Lr isotopes, as illustrated in Fig. 6. With this evidence in hand, we later performed a new series of bombardments to chemically separate and identify the source of these activities. Because of the 1000-fold larger cross sections for making 2.6-h ^{256}Fm, an interfering SF activity, it was necessary to perform two cation-exchange-column separations to achieve complete decontamination of the Lr isotopes. We made five bombardments ranging in length from 2 to 3 h, resulting in a new 39-min SF activity being found in the chemically separated Lr fractions. Decay analysis of the SF activity from these bombardments indicated there were two activities present, as shown in Fig. 7a. To confirm that the long-lived component was also a lawrencium activity and not from SF by ^{256}Fm, we performed three longer bombardments ranging from 5 to 21 h. The decay curve from one of these bombardments, shown in Fig. 7b, yielded a half-life of 212±18 min, while the average from the three experiments was 216 min. Later work indicated a half-life closer to 4 h.

The assignment of the 39-min activity to direct SF by ^{261}Lr rather than to its EC daughter, ^{261}No, is tenuous. Recent Q-value estimates for EC decay of ^{261}Lr span from 0.8 to 1.3 MeV. From the most reliable of these estimates, we would judge the EC half-life to be ~16 min. To test this possibility, we performed a series of chemical milking experiments in which nobelium was separated at 10-min intervals from a sample of purified lawrencium. No SF events were found in the No samples and, from this result, we calculate that the half-life for SF by ^{261}No, arising from the EC decay of ^{261}Lr, is less than 10 min. Unfortunately, a SF half-life for ^{261}No shorter than 10 min is still within expectations. Without the observation of ^{261}No, we were unable to demonstrate that the 39-min half-life was associated with EC decay by ^{261}Lr. As noted below, our efforts to establish the decay mode for ^{262}Lr were more successful.

e. ^{262}No

Estimated Q values for EC decay by 4-h ^{262}Lr are about 2 MeV, making EC decay to ^{262}No a definite possibility. Because SF by ^{262}No is unhindered by odd nucleons, its SF half-life was predicted to be as short nanoseconds or as long as a fraction of a second. Therefore, the 4-h decay period ascribed to ^{262}Lr might well represent EC decay by ^{262}Lr to produce ^{262}No, with the later being in secular equilibrium with its much longer-lived Lr parent. Thus, our experimental goals were to determine if ^{262}Lr decayed by EC and to measure the half-life and SF properties of it or its daughter, ^{262}No, by measuring the time intervals between nobelium K x-rays and subsequent SF events in samples of chemically purified lawrencium. For this purpose, we used the same specially constructed, high-geometry counter and attendant electronic and computer systems as were employed in searching for EC decay by ^{260}Md and in the successful finding of this decay mode for ^{258m}Md.[4]

A series of 38 bombardments, lasting from 2 to 9 h, of a 57-μg-cm^{-2} target of ^{254}Es with 127-MeV ^{22}Ne ions was made to produce ^{262}Lr. Recoil products caught on a Ta foil were chemically processed to remove fission products and nearby actinides from lawrencium. The pure Lr fraction was then electroplated on 27-μg-cm^{-2} polyimide foils that were overcoated with 25 μg-cm^{-2} of gold. The foils were placed between two large, unmounted surface-barrier detectors in a vacuum chamber with beryllium windows placed directly behind the surface-barrier detectors. Two large, intrinsic germanium detectors were inserted in back of these windows for detecting photons in the No K x-ray region.

The mean lifetime of ^{262}No and confirmation of ^{262}Lr EC decay to ^{262}No were derived from the distribution of logarithmic time intervals between photons having No K x-rays and subsequent fission events as shown in Fig. 8. Two distributions, which follow Poisson statistics, are resolved in the figure. The larger peak, with a mean lifetime of 1480 ms, is due to background photons preceding a fission event. We attribute the smaller peak at 6 ms to the mean lifetime of ^{262}No and some tailing of background events.[9] From the distribution of time intervals, we calculate a weighted average of 5 ms for the SF half-life of ^{262}No.

Correlated fission-fragment energies were determined by surface-barrier detectors during these experiments. From these, fragment mass and kinetic-energy distributions were calculated for ^{262}No and are described further in the following section. Its fission properties are characteristic of bimodal fission and are very similar to those found for ^{258}Fm and ^{260}Md. Observation of such an appreciable amount of the high-energy component is significant because this mode is thought to arise from the favorable division into Z=50, closed-shell Sn isotopes that are also near the 82-neutron closed shell. However, this nuclide lies two atomic numbers away

from Fm, so the proton division is not optimum. To account for the abundance of the high-energy mode, we believe the fragments' approach to the 82-neutron shell compensates for the unfavorable proton division. Heavier nuclei, provided they are neutron-rich, may similarly feature a significant "cold-fission" mode.

3. SPONTANEOUS-FISSION PROPERTIES: BIMODAL FISSION

Of the known isotopes of the elements from californium to the current limit at element 109, some 48 are known to decay, at least partially, by SF. Mass and kinetic-energy distributions have been measured for only about 18 of these nuclides (see Fig. 9) Until recently, this sort of significant information for transfermium nuclides was limited to ^{252}No (Ref 10) and ^{261}[105] (Ref 11). However, we expected fission studies in this region to be eventful for the reason that there was a sudden change in SF half-life systematics beginning with the isotopes of element 104. The cause was attributed to a sudden transformation of the fission barriers from a broad, double-humped one to a thinner, single barrier as seen in Fig. 10 for ^{260}[104]. The calculated one-dimensional barriers show the second or outermost barrier decreasing with increasing atomic number until it drops below the ground state around element 104, leaving only the inner barrier to be penetrated.[12,13] Theoretical calculations firmly predict the total disappearance of the outer barrier for isotopes of element 106 and beyond, although a second inner barrier begins to develop in this region due to splitting of the first barrier by hexadecapole deformation.[14]

Fission properties observed in the SF of the actinides lighter than Fm are characterized by highly asymmetrical mass distributions and average total-kinetic-energies (TKE) that gradually increase with the mass number of the fissioning species from ~174 to ~196 MeV. This trend continues into the lighter Fm isotopes until ^{258}Fm is reached. With this nuclide, an abrupt shift in properties occurs whereby the mass distribution becomes sharply symmetrical and the TKE jumps to 235 MeV. These features are illustrated in Figs. 11 and 12 for the isotopes of Cf and Fm.

With the benefit of new instruments and new, neutron-rich isotopes, we have extended these studies of fission properties to nuclei with higher atomic and neutron numbers.[9,15] Altogether, we have determined the mass and kinetic-energy distributions from the SF of ^{258}Fm, ^{259}Md, ^{260}Md, ^{252}No, ^{254}No, ^{258}No, ^{262}No, and ^{260}[104]. These mass and TKE distributions are pictured in Figs. 13 through 15. The overall trend is one in which mass asymmetry gives way to symmetrical mass division, and in the same region of nuclei, the fragment energies no longer fit a single distribution but consist of several distributions, indicating two or more modes of fission. These new forms of fission represents a rather startling and unexpected development based on

the fission behavior of all the other actinides. The question, of course, is why the earlier classical features of SF should so suddenly change with the addition of only a few nucleons.

The most significant and unique feature of these new TKE distributions (Figs. 14 and 15b) is their pronounced deviation from a single Gaussian shape typical of the TKE distributions from lighter actinide nuclei. In five of the six nuclides, decided asymmetry is imparted by conspicuous tailing in either energy direction from the central peak. Closer inspection of these TKE distributions reveals that the peak of each distribution is not randomly located along the energy axis, but is positioned near either 200 or 233 MeV. The asymmetrical tails of the TKE curves result in distributing an appreciable portion of the events into one or the other of these two main energy regions.

To account for these observations, we suggested that the TKE curves for at least five of the six nuclides were a composite of two separate energy distributions, with each being most likely Gaussian in shape.[15] The sixth nuclide, ^{260}[104], may have a residue of the high-energy component but the number of events was too small to tell. By using its distribution as a model for the low-energy component in the other five distributions, we resolved two Gaussian distributions from these five by least-mean-squares fitting with the results shown in Fig. 16. The reduced χ^2 values obtained from the fitting ranged from 0.55 to 1.32, values close enough to unity to indicate a reasonable probability of a good match in the fitting of two Gaussian's to the parent distributions. Largely on the basis of this evidence, we concluded there were low- and high-energy modes or bimodal fission occurring in five of the six nuclides studied.[15] Even though both modes were observed in the same nuclide, one generally predominated.

Because the high-energy component was unusually large in the fission of ^{260}Md, we have measured the neutron multiplicity in collaboration with colleagues at Philipps University, Marburg, FRG.[16] Previous studies of lighter actinides had demonstrated that the number of neutrons emitted per fission was proportional to the internal excitation energy of the ejected fragments. The high-energy mode of fission in ^{260}Md, averaging 234 MeV, leaves only ~21 MeV of excitation to be divided between the two fragments; thus, we expected a sharp decrease in the number of neutron emitted. In Fig. 17, we show the measured neutron-multiplicity and mass distributions for events with TKEs above 224 and below 210 MeV. This figure very graphically demonstrates that the large drop in the number of neutrons emitted by the high-energy mode is due to cold fragmentation, in which there is little excitation energy left in the fragments after scission to overcome the neutron binding energy. In-as-much as fragment excitation energy is correlated with deformation energy at scission, these neutron-multiplicity measurements imply nearly spherical fragments having little deformation.

Further sorting of SF events that lie within the subdistributions of TKEs shown in Fig. 16 delineate a relationship between mass and energy division that sheds additional information on the nature of these new kinds of SF. Based on conservation of momentum and the approximate conservation of mass, measurement of the kinetic energies of each of the fragments from a single SF event also provides the masses of the two fragments. The sum of the two fragments' energies gives the total kinetic energy. By selecting SF events that fall within a wide band of TKEs, the mass distributions associated with these chosen events can be obtained. Based on the extraction of two TKE distributions for ^{258}Fm, ^{259}Md, ^{260}Md, ^{258}No, and ^{262}No, we have arbitrarily taken 220 MeV as the dividing line between the low- and high-energy components. When the mass distributions for events lying above and below this energy are plotted (Fig. 18), it was found that the high-energy events yielded a sharply symmetrical mass distribution centered around A = 130. On the other hand, the low-energy fissions produced a broadly symmetrical distribution as seen in Fig. 18a. These correlations provide another distinguishing feature identifying two fission modes in addition to the distinct TKE distributions.

The cause of the high-energy, symmetrical-mass division in the heavy Fm, Md and No isotopes is believed to be strong shell effects in the emerging fission-product nuclei, which are driving the reaction toward the doubly magic ^{132}Sn nucleus.[17,18,19] Thus, the transition from asymmetrical mass division in the light fermium isotopes to symmetrical in the heavier ones would be due to fragments approaching closed proton and neutron shells (Z=50, N=82).[20] This explanation for the high-energy fission mode is in accord with the fading of this mode in ^{258}No and its near disappearance in ^{260}[104]. As the neutron number, N, decreases below 158 and the atomic number, Z, of the fissioning species increases beyond 100, the opportunity to divide into two fragments near the magic neutron and proton numbers diminishes. However, an equally satisfying explanation for the low-energy but still mass symmetrical fission mode, as represented by ^{260}[104], is less apparent. We have offered a rationale for the symmetrical mass distributions which is based on previous theoretical works that described the nuclear shapes favored at each of the fission barriers.[15] Theorists had found earlier that the outer hump of the double-humped barrier was reduced by 0.5 to 2 MeV when shapes from asymmetrical deformations were included in their calculations of the potential-energy surfaces (PES).[21] This reduction in barrier height is in comparison to calculations in which only symmetrical deformations were considered. When the outer barrier decreases and drops below the ground state, as indicated by SF half-lives and theoretically foreseen for the heaviest actinides,[13,22] then only the inner barrier favoring symmetrical shapes is penetrated in SF.

To account for the low, average TKE of about 200 MeV requires that the charge centers of the emerging fragments be somewhat further apart than for the high-energy mode in order to satisfy the observed Coulomb repulsion energies. This and the Q value of the reaction imply that the high-energy mode is compact and nearly spherical at the scission point, whereas the low-energy mode must be highly deformed and elongated when the fragments separate. Thus, the two distinct TKE distributions describe the nuclear shapes when the fissioning nuclide is close to rupturing into fragments, but they can not provide further details about the separate paths taken over the potential-energy landscape to reach this final stage of fission. Nonetheless, recent calculations of the PES have found appropriate paths that can account for two and even three separate modes of fission in very heavy nuclei.[23,24] A view of the new paths and valleys in the PES is given for ^{258}Fm in Fig. 19 (Ref.24). The paths correspond, going downwards in the figure, to the old path, a branch after the second barrier leading to elongated fragments, and one to compact spherical fragments. The old path refers to the single path derived before 1986 when only one mode of fission was thought to occur.

In contrast to the lighter actinides, where the differences in fission properties from one isotope to the next are subtle and nearly imperceptible (as seen in Figs. 11 and 12), the addition of a single nucleon results in abrupt and pronounced changes in the TKE and mass distributions. Adding a proton to ^{258}Fm causes the high-TKE mode to recede sharply in ^{259}Md, and the addition of a neutron to the latter nuclide brings about a sudden return of this mode in ^{260}Md. Such striking variations in fission properties undoubtedly reflect sharp changes in the internal structure of the nucleus brought about by shell effects. The alternative of assigning a predominant role to fragment properties in the case of ^{259}Md is difficult because there should be little difference in the fragments from this nuclide compared to those from the SF of its neighboring nuclei, ^{258}Fm, ^{259}Fm, and ^{260}Md. A further example of the erratic behavior of fission properties for nuclei in this region is the nonsystematic variation of SF half-lives with Z and N. Again, this behavior has been demonstrated to originate from shell corrections to the ground-state masses.

4. CONCLUSIONS

A surprising amount of information critical to advancing our theoretical understanding of the nucleus has resulted from the studies reported here. Chief among these is the observation of multiple fission modes. This finding has resulted in new insights into the fission process, greatly altering our perception of the physics involved, and some have thought it to be the most important discovery in fission within the last 20 years. The theoretical explanations for multiple paths over the potential-energy surface, if correct, allow us to speculate about the fission

properties of heavier nuclei. We expect the fission properties observed for ^{260}[104] to be typical of nuclides with equal or greater atomic numbers because of the disappearance of the outer barrier. However, it would not be surprising to find an intrusion of the high-energy mode as the neutron number approaches 164, with the consequent opportunity to divide into fragments with closed 82-neutron shells. We have found such a propensity in the SF properties of ^{262}No, but it is unknown as to the upward extent in Z that fragment-shell effects will continue to influence the fission process. Nevertheless, we suggest that the high-energy mode will disappear when strong fragment shells are no longer available.

Our experiments using ^{254}Es as a target have provided much needed knowledge on a group of neutron-rich and previously unknown nuclides lying in a critical region with respect to tests of theoretical predictions of SF half-lives. We note the finding of a reversal in the systematic trend of SF half-lives for the nobelium isotopes and, with each new isotope discovered, we have found SF half-lives to be five to ten orders of magnitude longer than anticipated ten years ago. This can be attributed to stabilization of the nuclear ground states by larger than expected strengths in both spin-orbit forces and pairing correlations. The fact that SF half-lives are much longer than expected is especially important because it now appears possible to extend the exploration of SF properties to nuclides that lie beyond those currently known. In addition, because of the sensitivity of fission properties to very small changes in barrier heights and intrinsic nuclear structure, accurate forecasting of the SF half-lives and properties of more distant and unknown nuclei still requires new experimental knowledge for normalization purposes.

Microscopic calculations of potential energy surfaces by Möller *et al.*,[25] Böning *et al.*,[26] and Cwiok *et al.*[27] show an improved stability for nuclides with N near 162 and atomic numbers between 106 and 110. Their calculations show the fission barriers increasing from about 5 MeV in the heavy actinides to 8.5 MeV in the center of this region because of a neutron subshell giving rise to a stable hexadecapole shape for the nucleus. It is especially important to determine whether these long theoretical extrapolations of nuclear properties are correct; if they are not, substantial changes in our understanding of the microscopic features of the nucleus would become necessary. For the near future, we believe the primary goal in heavy element research is to determine if the enormous increase in stability predicted for nuclei around this subshell exists. An experimental demonstration of these predictions is pivotal to further progress in reaching a fundamental understanding of the nucleus.

5 ACKNOWLEDGMENTS

The research work reported here was carried out by many scientists that have made up the the Heavy Element Group at the Lawrence Livermore National Laboratory, either as group members or as collaborators from other Laboratories. The list includes R. W. Lougheed, J. F. Wild, R. J. Dougan, K. J. Moody, J. H. Landrum, A. D. Dougan, C. M. Henderson, R. J. Dupzyk, R. L. Hahn, M. Schädel, K. Sümmerer, G. R. Bethune, J. van Aarle, W. Westmeier, D. C. Hoffman, K. E. Gregorich, C. M. Gannett, and R. A. Henderson. The bombardments were performed at the 88-in cyclotron at the Lawrence Berkeley Laboratory, for which we thank the staff for several thousand hours of heavy-ion beams. We are indebted for the use of the ^{254}Es target material to the Office of Basic Energy Sciences, U.S. Dept. of Energy, through the transplutonium productions facilities of the Oak Ridge National Laboratory. This research was performed under the auspices of the U.S. Department of Energy by the Lawrence Livermore National Laboratory under Contract No. W-7405-Eng-48.

REFERENCES

1. M. Schädel, W. Brüchle, M. Brügger, H. Gäggeler, K. J. Moody, D. Schardt, K. Sümmerer, E. K. Hulet, A. D. Dougan, R. J. Dougan, J. H. Landrum, R. W. Lougheed, J. F. Wild, and G. D. O'Kelley, Phys. Rev. C **33**, 1547 (1986).
2. R. W. Lougheed, J. H. Landrum, E. K. Hulet, J. F. Wild, R. J. Dougan, A. D. Dougan, H. Gäggeler, M. Schädel, K. J. Moody, K. E. Gregorich, and G. T. Seaborg, Phys. Rev. **32**, 1760 (1985).
3. D. C. Hoffman, J. B. Wilhelmy, J. Weber, W. R. Daniels, E. K. Hulet, R. W. Lougheed, J. H. Landrum, J. F. Wild, and R. J. Dupzyk, Phys. Rev. C **21**, 972 (1980).
4. E. K. Hulet, R. W. Lougheed, J. F. Wild, R. J. Dougan, K. J. Moody, R. L. Hahn, C. M. Henderson, R. J. Dupzyk, and G. R. Bethune, Phys. Rev. C **34**, 1394 (1986).
5. E. K. Hulet, J. F. Wild, R. W. Lougheed, J. E. Evans, B. J. Qualheim, M. Nurmia, and A Ghiorso, Phys. Rev Lett. **26**, 523 (1971).
6. L. P. Somerville, M. J. Nurmia, J. M. Nitschke, A. Ghiorso, E. K. Hulet, and R. W. Lougheed, Phys. Rev. C **31**, 1801 (1985).
7. K. J. Moody, R. W. Lougheed, R. J. Dougan, E. K. Hulet, J. F. Wild, K. Sümmerer, R. L. Hahn, J. van Aarle, and G. R. Bethune, Phys. Rev. C **41**, 152 (1990).
8. R. W. Lougheed, E. K. Hulet, R. J. Dougan, J. F. Wild, R. J. Dupzyk, C. M. Henderson, K. J. Moody, R. L. Hahn, K. Sümmerer, and G. Bethune, J. Less-Common Met. **122**, 461 (1986).

9. R. W. Lougheed, E. K. Hulet, J. F. Wild, K. J. Moody, R. J. Dougan, C. M. Gannett, R. A. Henderson, D. C. Hoffman, and D. M. Lee, *Nuclear Chemistry Division FY-88 Annual Report*, Lawrence Livermore National Laboratory, Report No. UCAR 10062/88, 1988 (unpublished), p. 135; E. K. Hulet, presented at the Conference on Fifty Years with Nuclear Fission, Washington, DC, April 26-28, 1989, in *50 Years with Nuclear Fission*, edited by J. W. Behrens and A. D. Carlson (Am Nuclear Soc., La Grange Park, Illinois, 1989), Vol. II, p. 533.
10. C. E. Bemis, Jr., R. L. Ferguson, F. Plasil, R. J. Silva, F. Pleasonton, and R. L. Hahn, Phys. Rev. C **15**, 705 (1977).
11. C. E. Bemis, Jr., R. L. Ferguson, F. Plasil, R. J. Silva, G. D. O'Kelley, M. L. Kiefer, R. L. Hahn, D. C. Hensley, E. K. Hulet and R. W. Lougheed, Phys. Rev. Lett. **39**, 1246 (1977).
12. J. Randrup, C. F. Tsang, P. Möller, S. G. Nilsson, and S. E. Larsson, Nucl. Phys. **A217**, 221 (1973).
13. J. Randrup, S.E. Larsson, P Möller, S. G. Nilsson, K. Pomorski, and A. Sobiczewski, Phys. Rev. C **13**, 229 (1976).
14. S. Cwiok, V.V. Pashkevich, J. Dudek, and W. Nazarewicz, Nucl. Phys. **A410**, 254 (1983).
15. E. K. Hulet, J. F. Wild, R. J. Dougan, R. W. Lougheed, J. H. Landrum. A. D. Dougan, P. A. Baisden, C. M. Henderson, R. J. Dupzyk, R. L. Hahn, M. Schädel, K Sümmerer, and G. R. Bethune, Phys. Rev. C **40**, 770 (1989); E. K. Hulet, J. F. Wild, R. J. Dougan, R. W. Lougheed, J. H. Landrum. A. D. Dougan, M. Schädel, R. L. Hahn, P. A. Baisden, C. M. Henderson, R. J. Dupzyk, K Sümmerer, and G. R. Bethune, Phys. Rev. Lett. **56**, 313 (1986).
16. J. F. Wild, J. van Aarle, W. Westmeier, R. W. Lougheed, E. K. Hulet, K. J. Moody, R. J. Dougan, R. Brandt, E.-A. Koop, and P. Patzelt, Phys. Rev. C **41**, 640 (1990).
17. J. R. Nix, Annual Rev. Nucl. Sci. **22**, 341 (1972).
18. U. Mosel, J. Maruhn, and W. Greiner, Phys. Lett. **34B**, 587 (1971).
19. U. Mosel and H. W. Schmitt, Phys. Rev. C **4**, 2185 (1971).
20. M. G. Mustafa, U. Mosel, and H. W. Schmitt, Phys. Rev. Lett. **28**, 1536 (1972); M. G. Mustafa, U. Mosel, and H. W. Schmitt, Phys. Rev. C **7**, 1519 (1973).
21. P. Möller and S. G. Nilsson, Phys. Lett. **31B**, 283 (1970) 283; H. C. Pauli, T. Ledergerber, and M. Brack, Phys. Lett. **34B**, 264 (1971); G. Gustafsson, P Möller, and S. G. Nilsson, Phys. Lett. **34B**, 349 (1971).
22. A. Baran, K. Pomorski, A. Lukasiak, and A. Sobiczewski, Nucl Phys. **A361**, 83 (1981); H. C. Pauli and T. Ledergerber, in *Proceedings of the Symposium on the Physics and Chemistry of Fission*, Rochester, New York, 1973 (International Atomic Energy Agency, Vienna, Austria, 1974), Vol. I, p. 463.

23. U. Brosa, S. Grossmann, and A. Müller, Z. Phys. A **325**, 242 (1986); V. V. Pashkevich and A. Sandulescu, Rapid Communications No. 16-86, Joint Institute for Nuclear Research, Dubna, USSR (1986), p. 19-23; K. Depta, J. A. Maruhn, W. Greiner, W. Scheid, and A. Sandulescu, Mod. Phys. Lett. A **1**, 377 (1986); V. V. Pashkevich, Nucl. Phys. **A477**, 1 (1988); S. Cwiok, P. Rozmej, and A. Sobiczewski, in AIP Conf. Proc. No. 164, *5th Int. Conf. on Nuclei far from Stability*, Lake Rosseau, Canada, 1987, edited by I. S. Towner (Am. Inst. Physics, New York, 1988) p. 821; S. Cwiok, P. Rozmej, A. Sobiczewski, and Z. Patyk, Nucl. Phys. **A411** 281 (1989).

24. P. Möller, J. R. Nix, and W. J. Swiatecki, Nucl. Phys. **A469**, 1 (1987); P. Möller, J. R. Nix, and W. J. Swiatecki, Nucl. Phys. **A492**, 349 (1989); P. Möller, J. R. Nix, and W. J. Swiatecki, presented at the Conference on Fifty Years with Nuclear Fission, Washington, DC, April 25-28, 1989, in *50 Years with Nuclear Fission*, edited by J. W. Behrens and A. D. Carlson (Am. Nuclear Soc., La Grange Park, Illinois, 1989), Vol I, p. 153.

25. P. Möller, J. R. Nix, W. D. Myers, and W. J. Swiatecki, *Proc. 4th Winter Workshop on Nuclear Dynamics*, Copper Mt., Colorado, February 22—28, (1986).

26. K. Böning, Z. Patyk, A. Sobiczewski, and S. Cwiok, Z. Phys. **A325**, 479 (1986).

27. S. Cwiok, V. V. Pashkevich, J. Dudek, and W. Nazarewicz, Nucl. Phys. **A410**, 254 (1983).

FIGURE CAPTIONS

FIG. 1. A portion of the nuclide chart showing the isotopes produced in bombardments of ^{254}Es. Those shaded were discovered in ^{254}Es bombardments, while those enclosed in a border represent attempts to identify their formation. The long arrow indicates the peak of mass flow in transfer reaction.

FIG. 2. Isotopic yield distributions measured for the reactions of (a) 105-MeV ^{18}O and (b) 125 and 126 MeV ^{22}Ne with ^{254}Es. Cross sections from Ref. 1 with the addition of those for the new isotopes, ^{261}Lr and ^{262}Lr, in b.

FIG. 3. Logarithmic time distributions for the last energy-windowed photon detected before SF of ^{258}Fm. The photon energy window corresponds to the K x-ray region of Fm (112—145 keV). In this figure, the occurrence of fission is defined as zero time. The distribution around 520 μs before fission is the lifetime of ^{258}Fm (Ref. 4).

FIG. 4. Isotopic yields from transfer reactions in 72-MeV ^{13}C bombardments of ^{254}Es (Ref. 7).

FIG. 5. Composite decay curve for ^{260}Md obtained by counting two samples for 7 months.

FIG. 6. Decay properties we estimated for ^{261}Lr and ^{262}Lr but with the inclusion of our measured values for the SF half-life of ^{261}Lr and the EC half-life of ^{262}Lr.

FIG. 7. (a) Composite SF decay curve from chemically isolated Lr produced from four, 2-h bombardments of ^{254}Es with 127-MeV ^{22}Ne ions. A 39-min and a 200- to 300-min component were observed. (b) Decay curve for the longer-lived SF activity found in Lr fractions from a 10-h bombardment.

FIG. 8. The logarithmic distribution of time intervals between the last photon with No K x-ray energies preceding a SF event. The smooth curves are exponential fits to the measured data shown by the histogram.

FIG. 9. Portion of the Nuclide Chart showing isotopes known to decay by spontaneous fission. Shading of a nuclide indicates the mass and kinetic-energy distributions have now been determined.

FIG. 10. Fission barriers calculated with single-particle and pairing corrections to the liquid-drop barrier. After Randrup *et al.* (Refs. 12 and 13).

FIG. 11. Mass distributions of the fragments obtained in the spontaneous fission of Cf and Fm isotopes. Until ^{258}Fm is reached, only slight differences are found in the asymmetrical mass distributions. An abrupt transformation to sharply symmetrical mass distributions occurs at ^{258}Fm.

FIG. 12. Total-kinetic-energy distributions for the fragments from the spontaneous fission of Cf and Fm isotopes. The average TKEs modestly increase with increasing atomic number up to ^{258}Fm, where a sudden increase of ~40 MeV is apparent.

FIG. 13. Provisional mass distributions (no neutron corrections) obtained from correlated fragment energies. The mass bins have been chosen to be slightly different for each nuclide. The distributions are net after subtracting a small ^{256}Fm component. From Ref. 15.

FIG. 14. Provisional total-kinetic-energy distributions. A small contribution equivalent to the known amount of ^{256}Fm has been subtracted from all but the the ^{260}Md distribution. From Ref. 15.

FIG. 15. (a) Provisional mass distribution obtained for 5-ms ^{262}No; (b) Total-kinetic-energy distribution from the spontaneous fission of ^{262}No. Dashed curves are unfolding of the TKE distribution into two Gaussians by least-mean-squares fitting. From Ref. 9.

FIG. 16. Unfolding of the asymmetric TKE distributions of Figs. 14 and 15b into two Gaussian's by least-mean-squares fitting. From Refs. 15 and 9.

FIG. 17. Lower figure: Neutron multiplicity distributions from the SF of ^{260}Md correlated with the total-kinetic-energies of the fragments. The dashed histogram is associated with TKEs above 224 MeV while the solid-lined one belongs to events with TKEs less than 210 MeV. Upper figure: Mass distributions related to the same TKE bins. From Ref. 16.

FIG. 18. Mass distributions obtained by sorting fission events according to their total kinetic energies: (a) for events with TKEs less than 220 MeV and (b) for those with TKEs $\geq$ 220 MeV. From Refs. 15 and 9.

FIG. 19. Potential-energy surface for ^{258}Fm. Two valleys exiting toward scission are found after the small second barrier near the center of the figure. The paths indicated on the figure show the possible minimum potential-energy trajectories. These paths correspond, going downward, to the old path, a path after the second barrier leading to elongated fragments, and a new path that results in compact, spherical fragments. From Ref. 24.

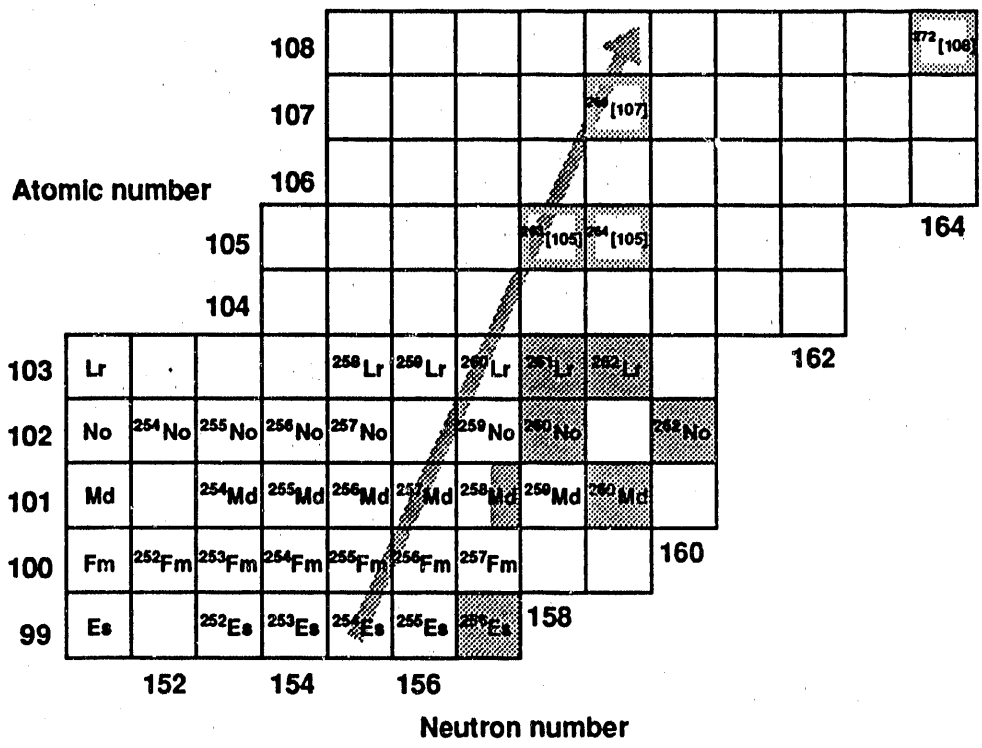
Atomic number
108
107
106
105
104
103
102
101
100
99
Lr
No
Md
Fm
Es
^{254}No
^{255}No
^{256}No
^{257}No
^{259}No
^{260}No
^{262}No
^{254}Md
^{255}Md
^{256}Md
^{257}Md
^{258}Md
^{259}Md
^{260}Md
^{252}Fm
^{253}Fm
^{254}Fm
^{255}Fm
^{256}Fm
^{257}Fm
^{252}Es
^{253}Es
^{254}Es
^{255}Es
^{256}Es
^{258}Lr
^{259}Lr
^{260}Lr
^{261}Lr
^{262}Lr
^{264}[105]
^{264}[107]
^{272}[108]
152
154
156
158
160
162
164
Neutron number

Fig. 1

Yields from ^{18}O and ^{22}Ne Reactions with ^{254}Es

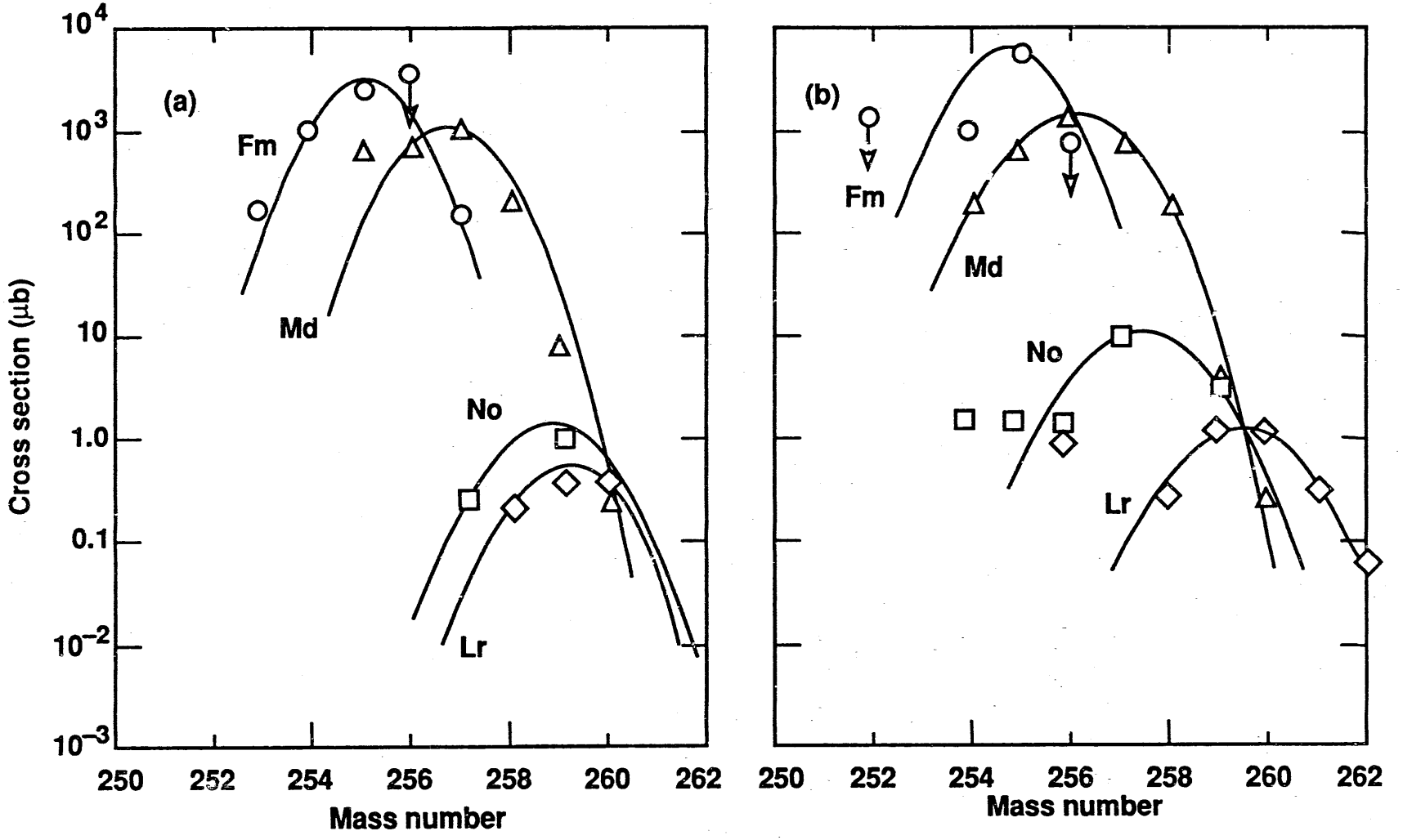

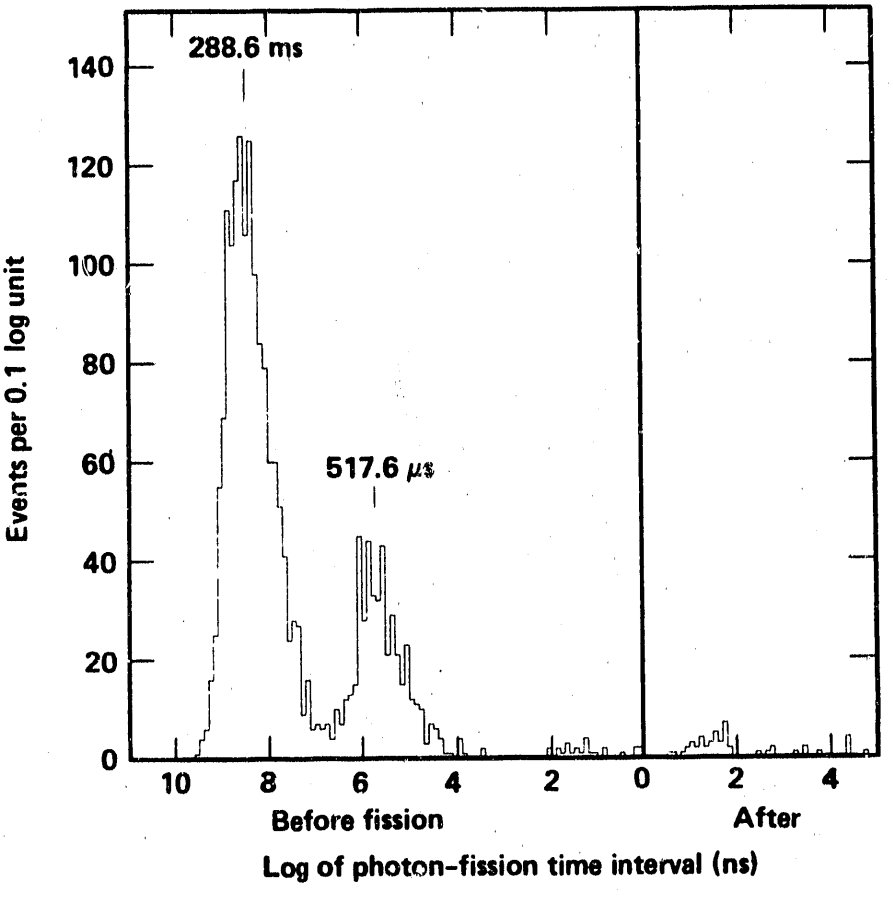
288.6 ms
517.6 μs
140
120
100
80
60
40
20
0
Events per 0.1 log unit
10
8
6
4
2
0
2
4
Before fission
After
Log of photon-fission time interval (ns)

Fig 3

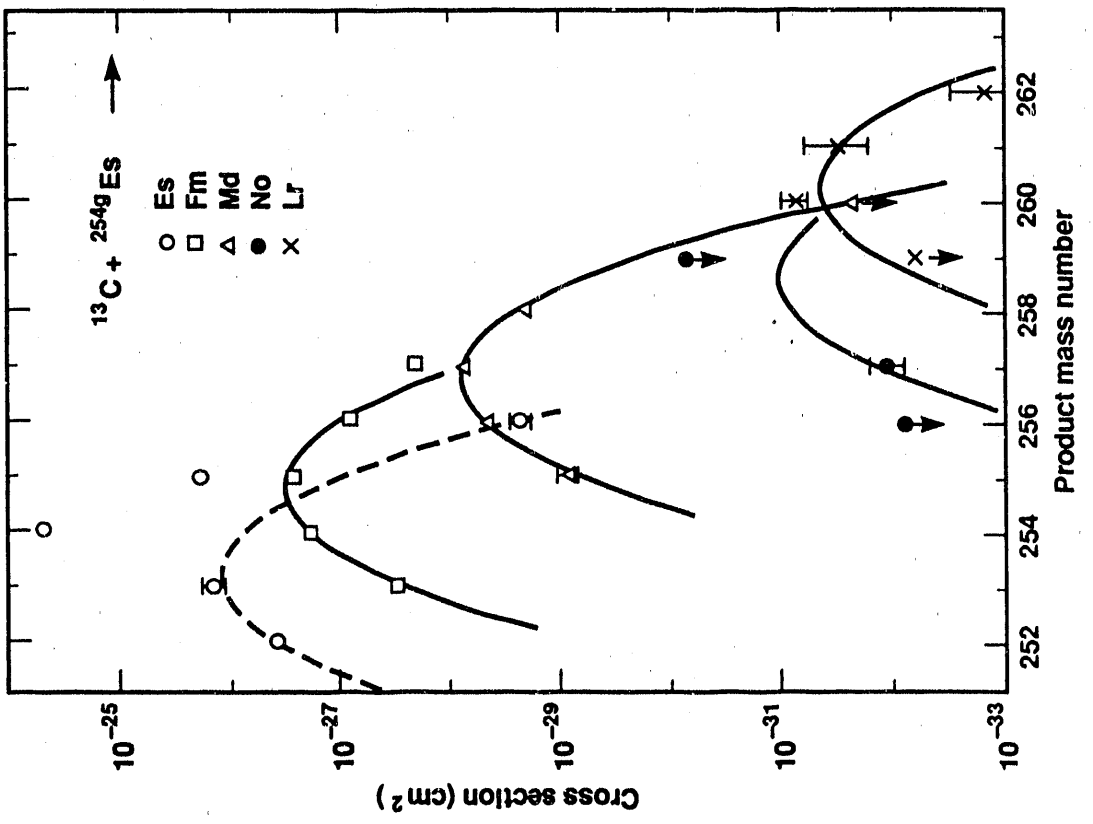
$^{13}C + ^{254g}Es$
Es
Fm
Md
No
Lr
Cross section (cm^2)
10^{-25}
10^{-27}
10^{-29}
10^{-31}
10^{-33}
252
254
256
258
260
262
Product mass number

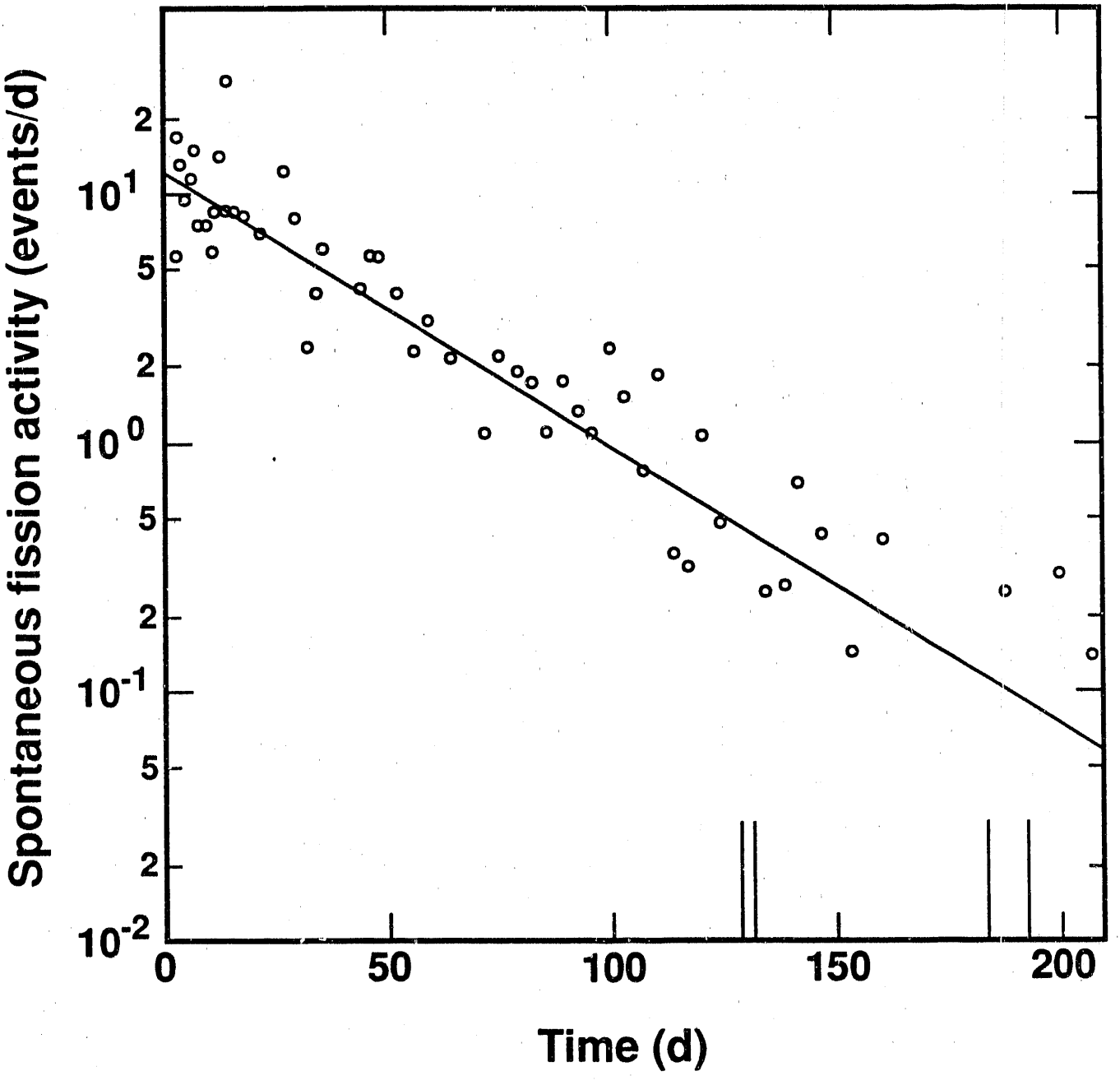
Spontaneous fission activity (events/d)
2
10^1
5
2
10^0
5
2
10^-1
5
2
10^-2
0
50
100
150
200
Time (d)

Fig 5

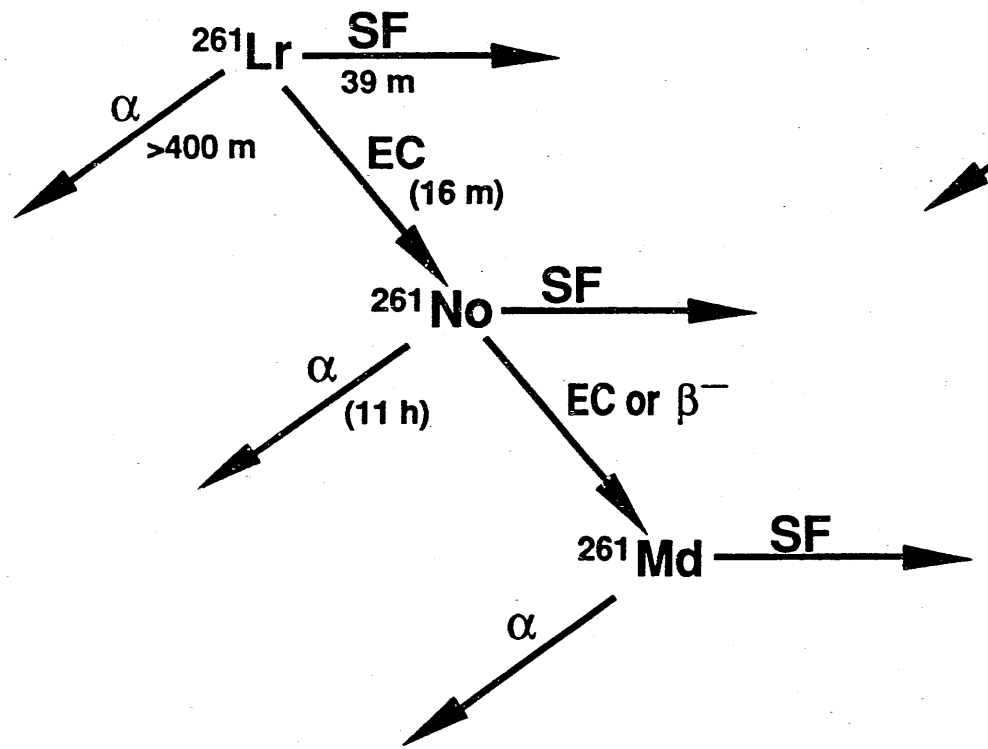
261Lr
SF
39 m
α
>400 m
EC
(16 m)
261No
SF
α
(11 h)
EC or β−
261Md
SF
α

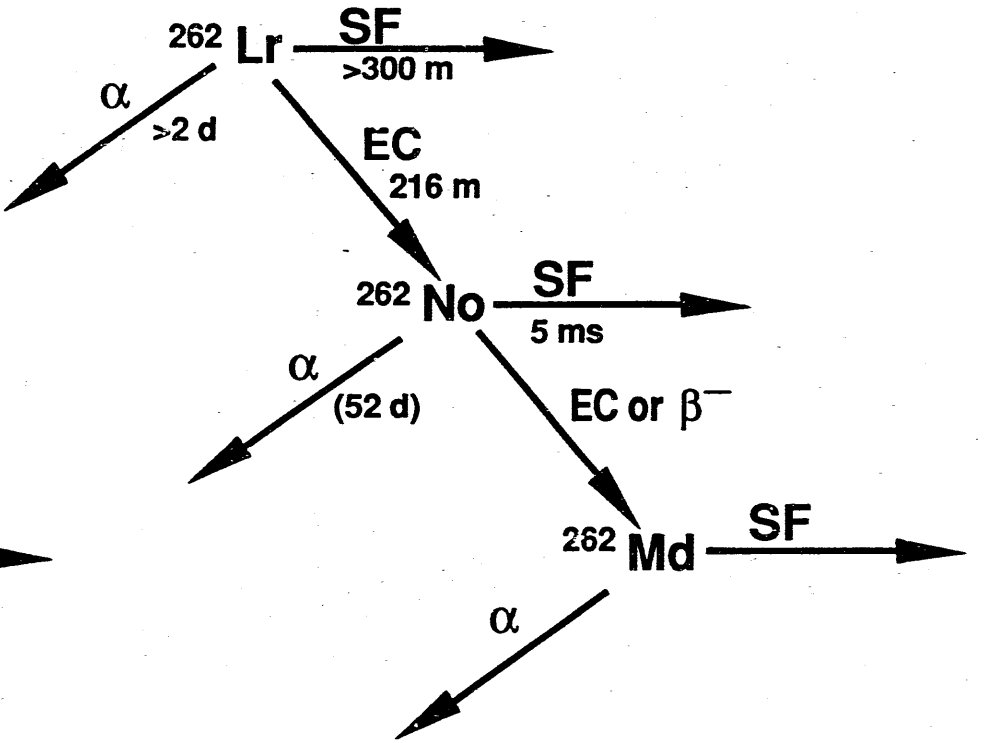
262 Lr
SF
>300 m
α
>2 d
EC
216 m
262 No
SF
5 ms
α
(52 d)
EC or β−
262 Md
SF
α

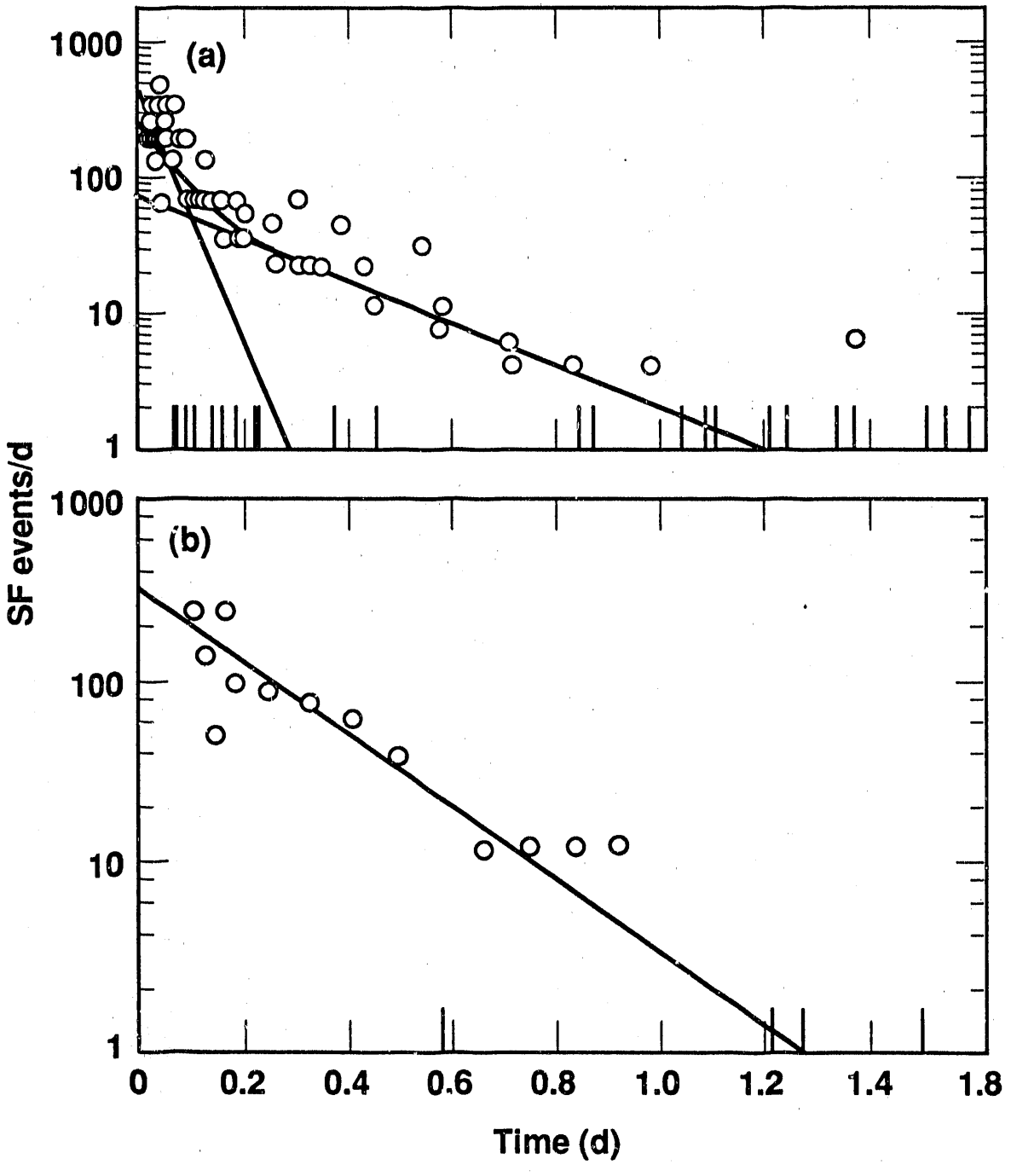

MG-L-U-6867-06

Fig 7

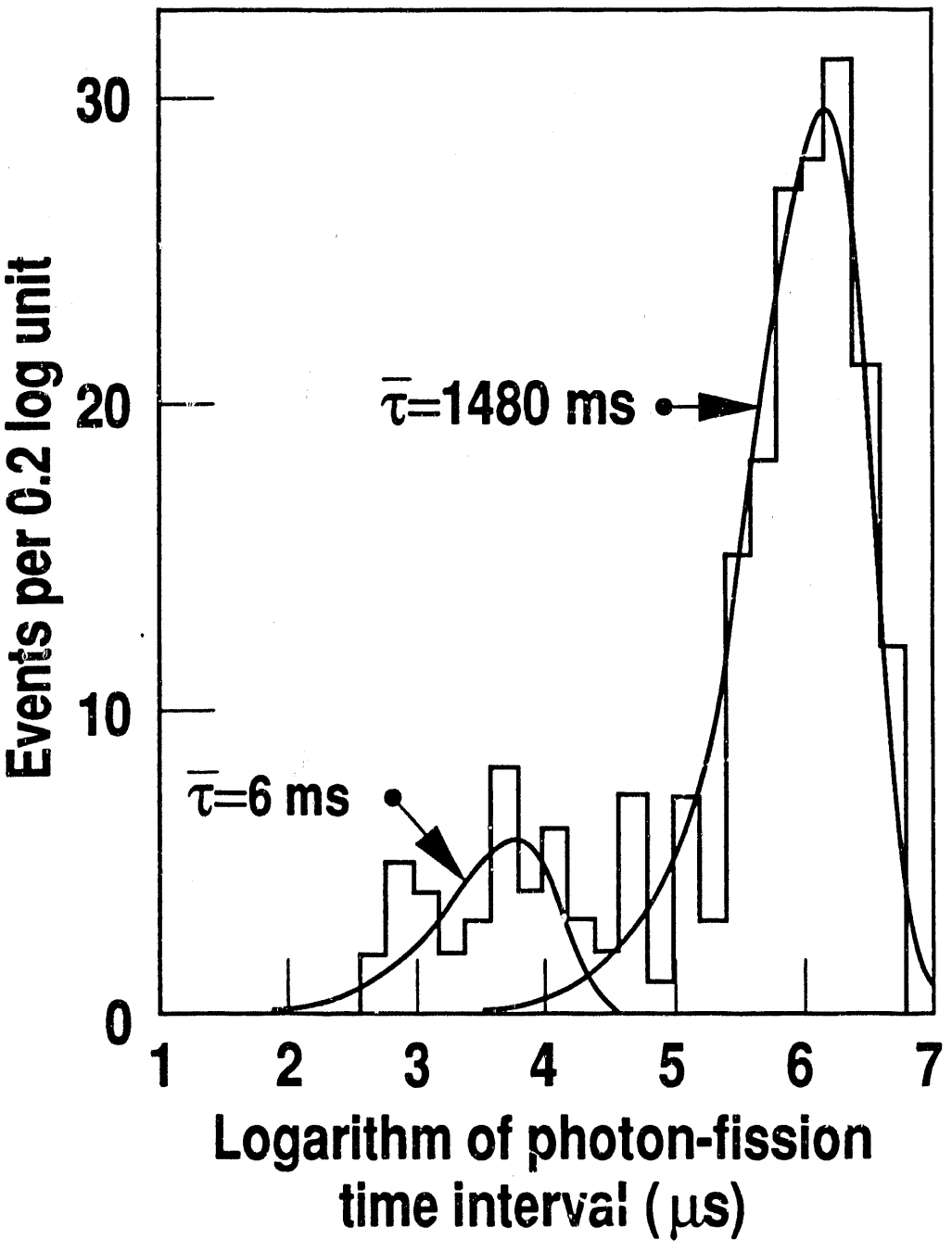
30
20
10
0
Events per 0.2 log unit
$\bar{\tau}$=1480 ms
$\bar{\tau}$=6 ms
1
2
3
4
5
6
7
Logarithm of photon-fission time interval (μs)

Fig 8

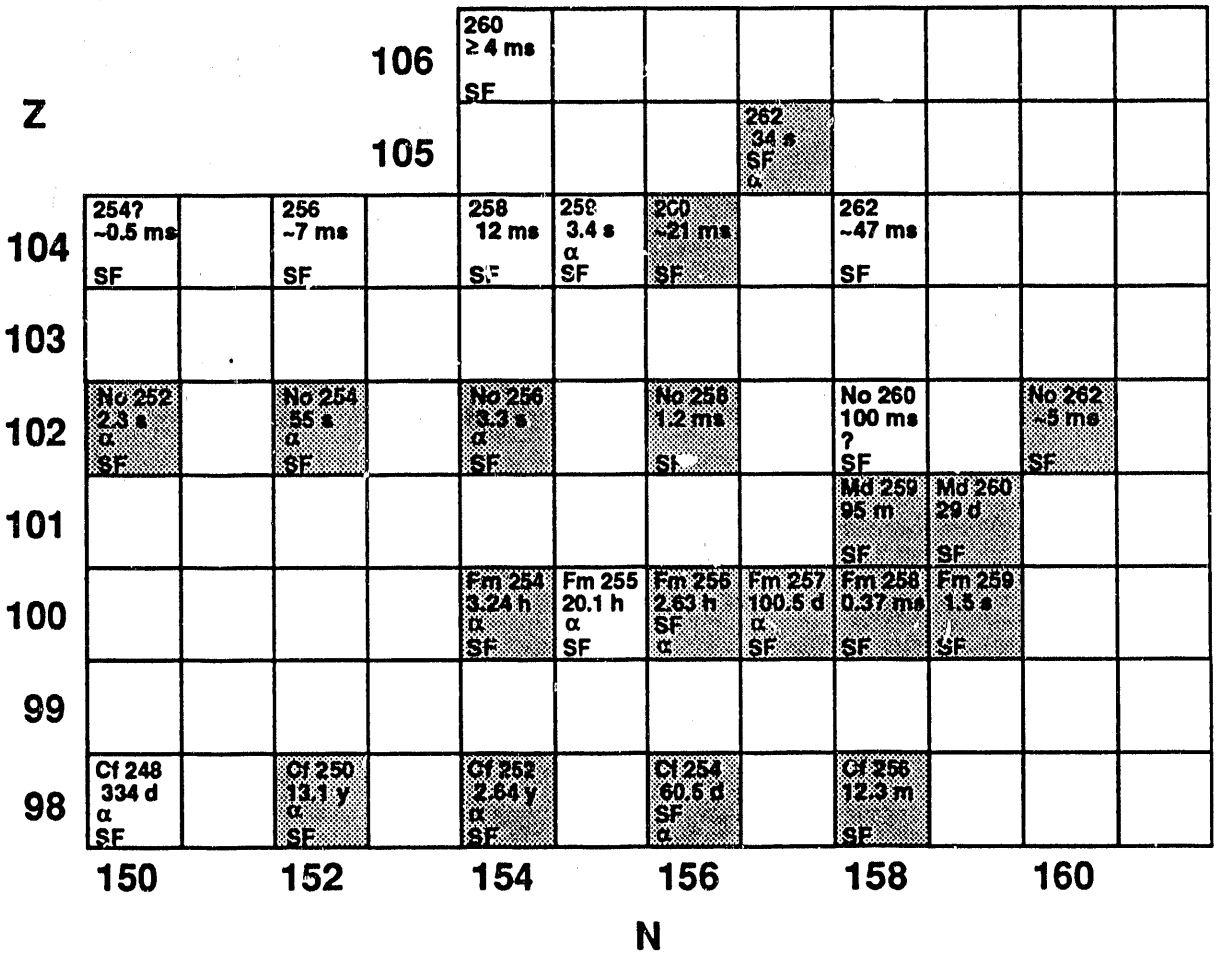
Z
106
105
104
103
102
101
100
99
98
260 ≥ 4 ms SF
262 34 s SF α
254? ~0.5 ms SF
256 ~7 ms SF
258 12 ms SF
258 3.4 s α SF
260 ~21 ms SF
262 ~47 ms SF
No 252 2.3 s α SF
No 254 55 s α SF
No 256 3.3 s α SF
No 258 1.2 ms SF
No 260 100 ms ? SF
No 262 ~5 ms SF
Md 259 95 m SF
Md 260 29 d SF
Fm 254 3.24 h α SF
Fm 255 20.1 h α SF
Fm 256 2.63 h SF α
Fm 257 100.5 d α SF
Fm 258 0.37 ms SF
Fm 259 1.5 s SF
Cf 248 334 d α SF
Cf 250 13.1 y α SF
Cf 252 2.64 y α SF
Cf 254 60.5 d SF α
Cf 256 12.3 m SF
150
152
154
156
158
160
N

Fig. 9

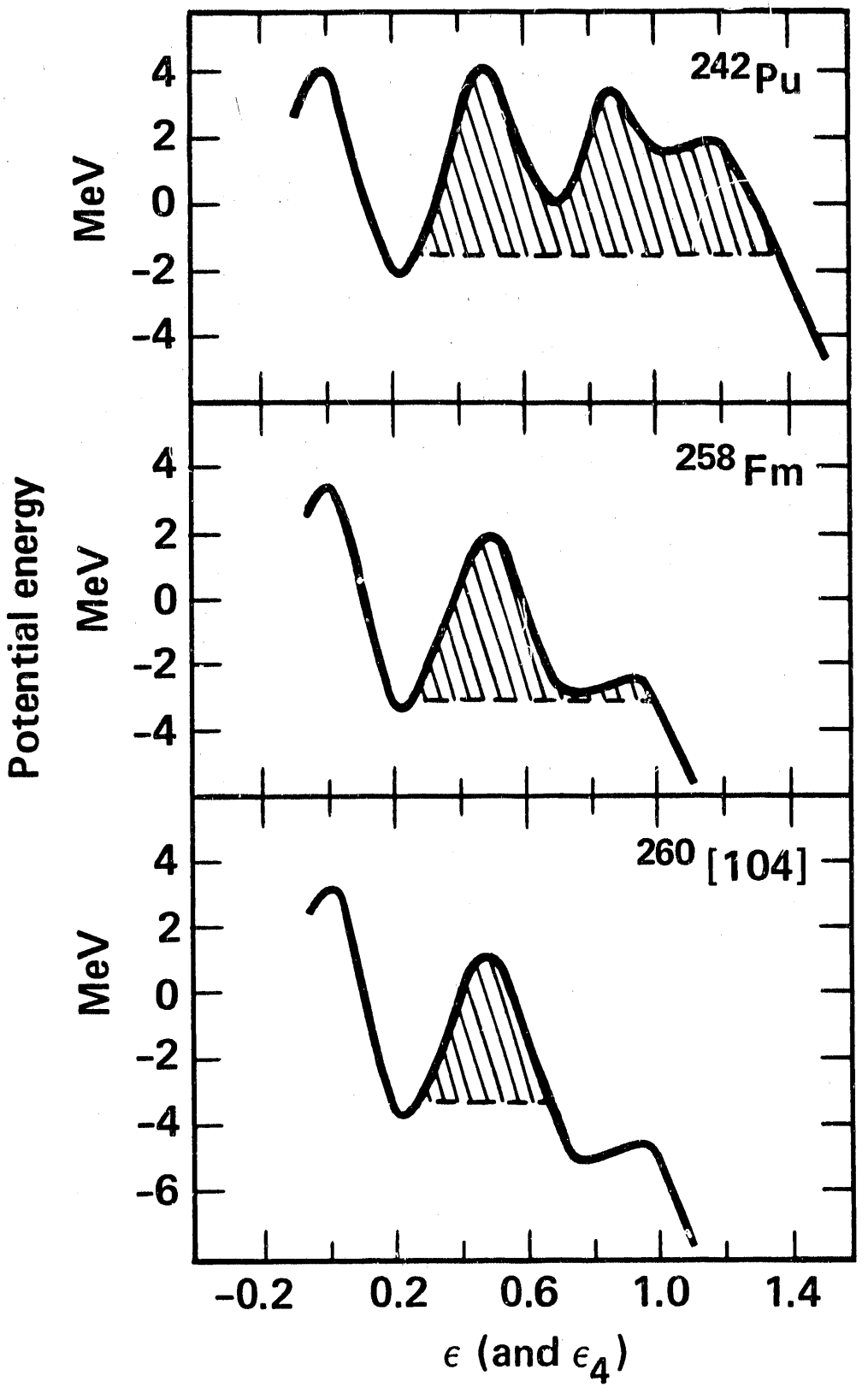
Potential energy
MeV
4
2
0
-2
-4
^{242}Pu
^{258}Fm
^{260} [104]
-6
-0.2
0.2
0.6
1.0
1.4
ϵ (and ϵ_4)

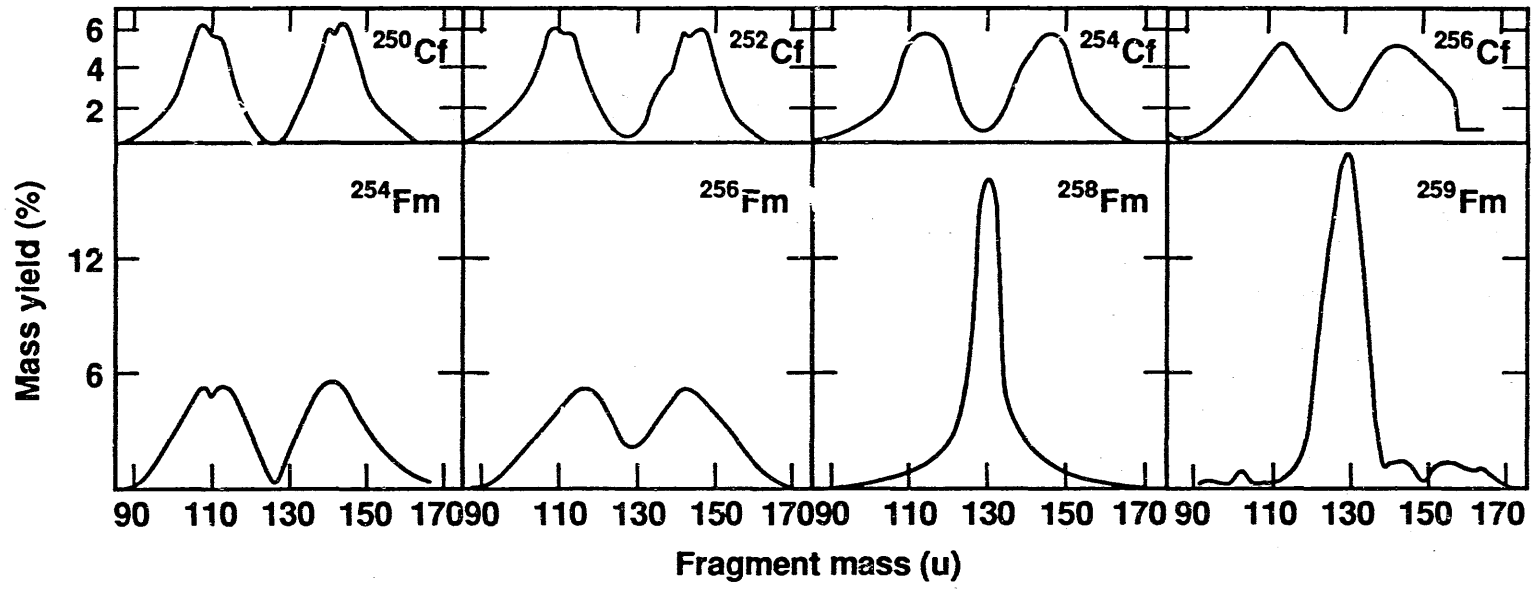

RRN-AS16-U-6932-2

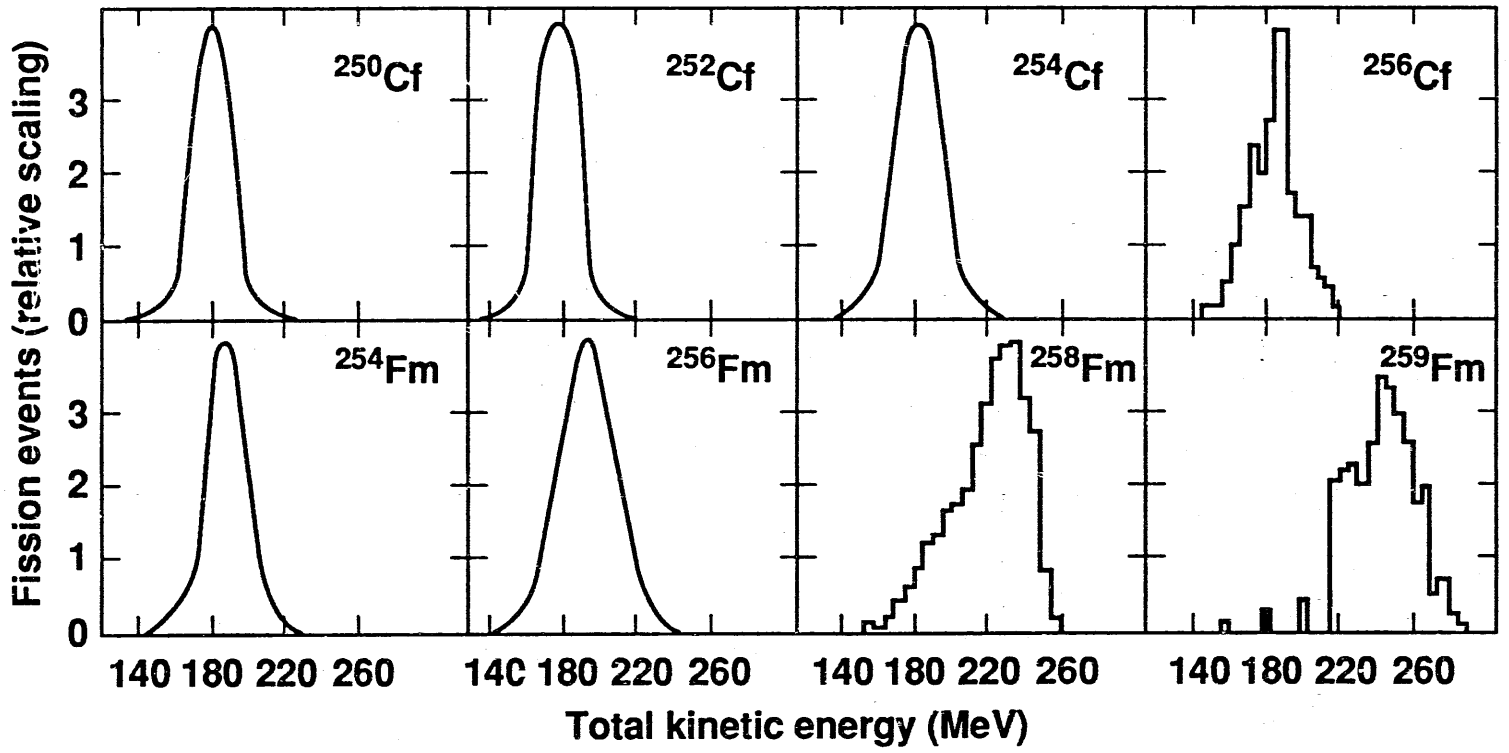

PT-AS11-U-6932-1

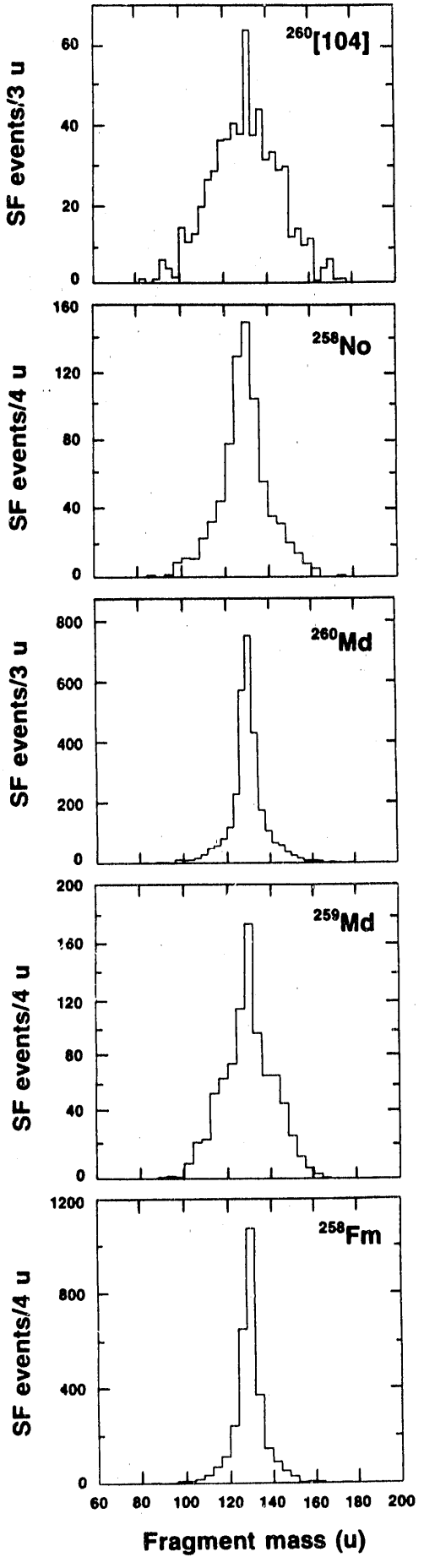
^{260}[104]
SF events/3 u
^{258}No
SF events/4 u
^{260}Md
SF events/3 u
^{259}Md
SF events/4 u
^{258}Fm
SF events/4 u
Fragment mass (u)

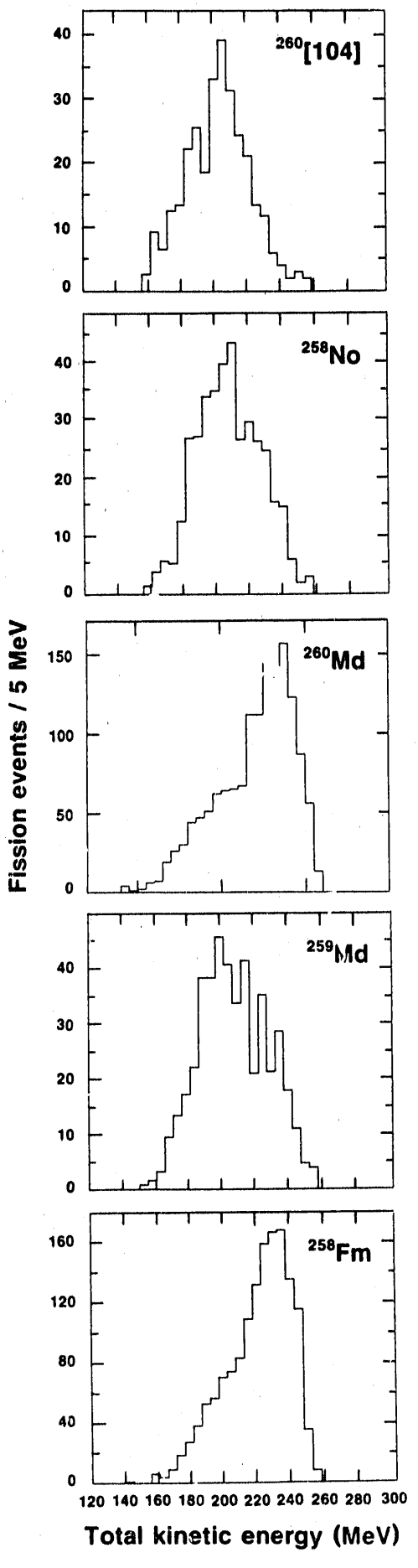
^{260}[104]
^{258}No
^{260}Md
^{259}Md
^{258}Fm
Fission events / 5 MeV
Total kinetic energy (MeV)
120 140 160 180 200 220 240 260 280 300

Fig 14

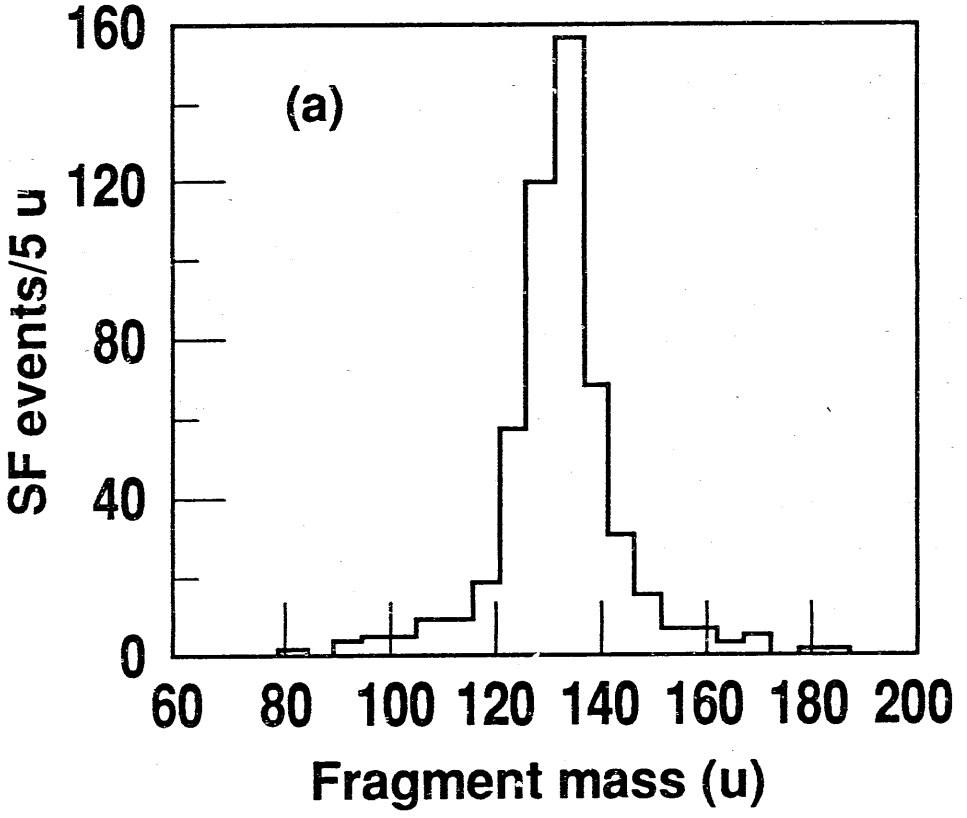
(a)
SF events/5 u
160
120
80
40
0
60
80
100
120
140
160
180
200
Fragment mass (u)

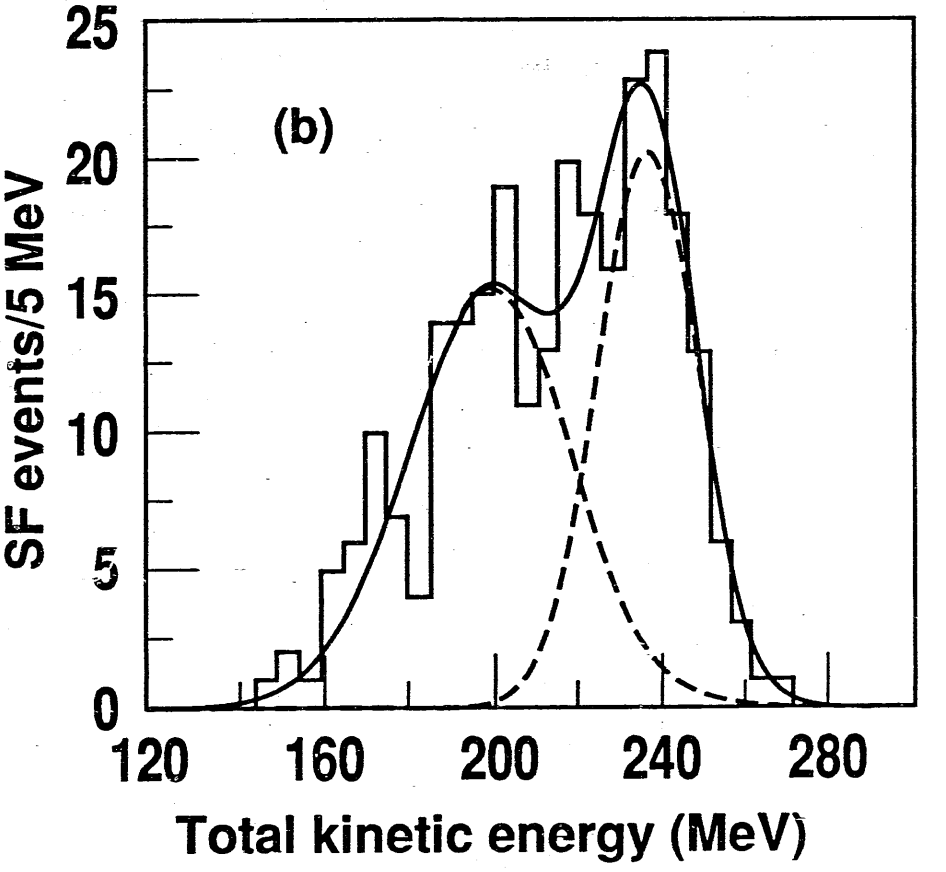
(b)
SF events/5 MeV
25
20
15
10
5
0
120
160
200
240
280
Total kinetic energy (MeV)

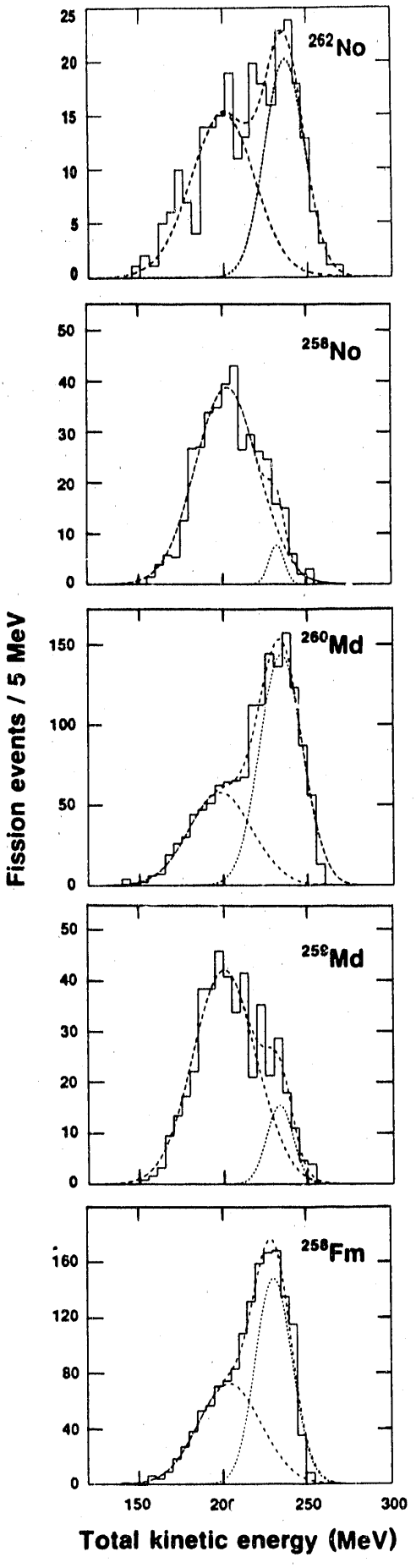
^{262}No
^{258}No
^{260}Md
^{259}Md
^{258}Fm
Fission events / 5 MeV
Total kinetic energy (MeV)

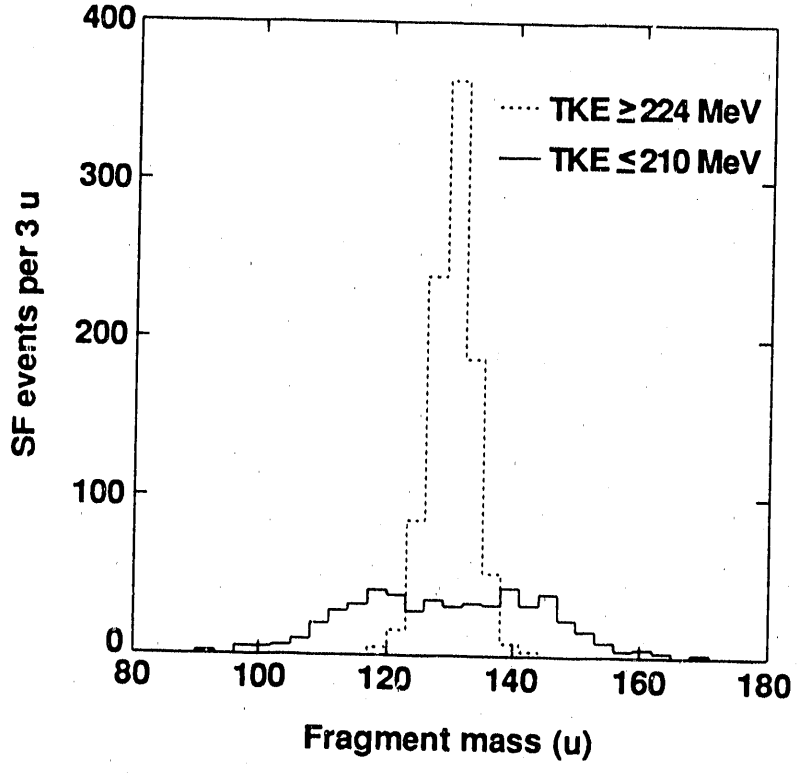
400
300
200
100
0
80
100
120
140
160
180
SF events per 3 u
Fragment mass (u)
TKE ≥ 224 MeV
TKE ≤ 210 MeV

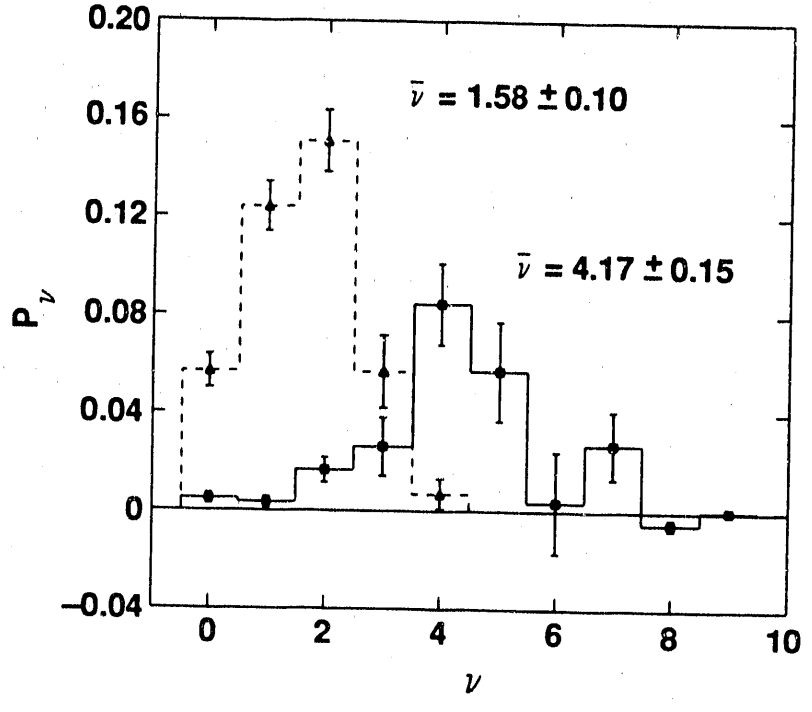
0.20
0.16
0.12
0.08
0.04
0
−0.04
0
2
4
6
8
10
P_ν
ν
$\bar{\nu}$ = 1.58 ± 0.10
$\bar{\nu}$ = 4.17 ± 0.15

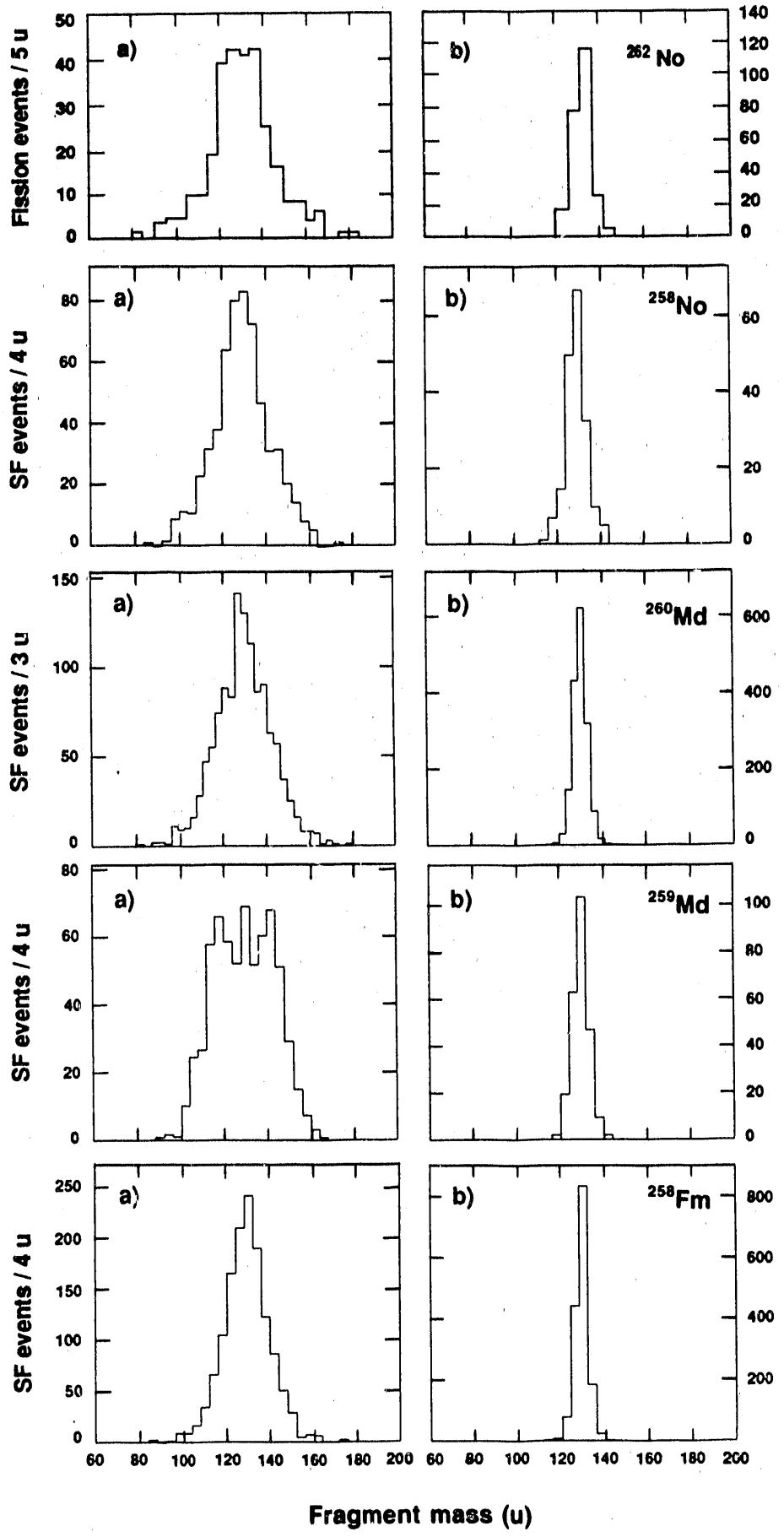
a)
b)
^{262}No
^{258}No
^{260}Md
^{259}Md
^{258}Fm
Fission events / 5 u
SF events / 4 u
SF events / 3 u
SF events / 4 u
SF events / 4 u
Fragment mass (u)

Fig 18

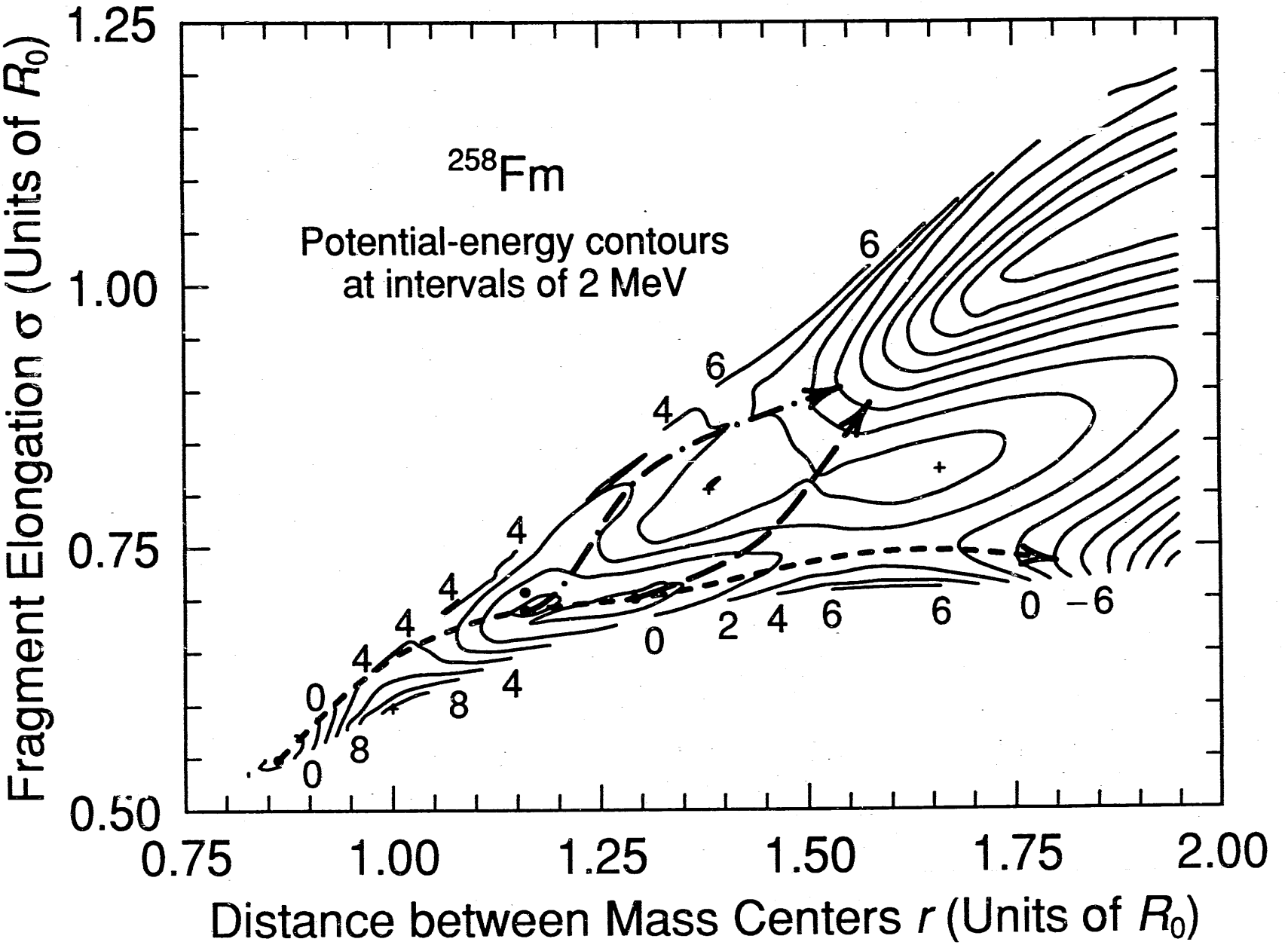
^{258}Fm
Potential-energy contours
at intervals of 2 MeV
Fragment Elongation σ (Units of R_0)
Distance between Mass Centers r (Units of R_0)
1.25
1.00
0.75
0.50
0.75
1.00
1.25
1.50
1.75
2.00
6
6
4
4
4
4
4
4
0
2
4
6
6
0
−6
0
8
0
8
4

END

DATE FILMED

02/26/91